An h/p adaptive DG method for shock dominated high speed flows

John Ekaterinaris

and

Konstantinos Panourgias

Embry-Riddle Aeronautical University

Daytona Beach FL

Applied Modeling & Simulation (AMS) Seminar Series
NASA-Ames Research Center, Nov. 25, 2014



ERAU

Outline of the Presentation

- Motivation and Objectives
- Numerical Method
- Validation of the Method
- Results with AMR and h/p refinement
- Conclusions



ERAU

Motivation and Objectives

- To develop a unified limiting approach for all types of three dimensional elements for P1 DG expansions with p-adaptive capabilities away from discontinuities
- To develop dynamic AMR capabilities and the ability to use higher order expansions (P2 or higher) away from discontinuities based on computed flow features.
- To advance implicitly in time the full coupled system
- To apply and demonstrate dynamic AMR and dynamic h/p refinement for time dependent complex flow problems.

DG discretization

ERAU

$$\frac{\partial U}{\partial t} + div\,\bar{\bar{Q}} = S$$

- Weak form of the system

$$\int_{\Omega} \Phi \frac{\partial \boldsymbol{U}}{\partial t} d\Omega = \int_{\Omega} \nabla\Phi \cdot \boldsymbol{Q}(\boldsymbol{U}, \nabla \boldsymbol{U})\, d\Omega - \int_{\partial\Omega} \Phi \boldsymbol{Q}(\boldsymbol{U}, \nabla \boldsymbol{U}) \cdot \boldsymbol{n}\, dA + \int_{\Omega} \Phi \cdot \boldsymbol{S}(\boldsymbol{U})\, d\Omega$$

- Use the same polynomial spaces for weighting and expansion functions
- The approximate solution is $\boldsymbol{U}_h = \sum_i c_i \Phi_i$ and the discrete weak form becomes

$$\mathrm{M} \frac{\partial \mathbf{c}}{\partial t} = \int_K \nabla\Phi_i \cdot \boldsymbol{Q}(\boldsymbol{U}_h, \nabla \boldsymbol{U}_h)\, dK - \int_{S_K} \Phi_i \widehat{\boldsymbol{Q}}(\boldsymbol{U}_h, \nabla \boldsymbol{U}_h) \cdot \boldsymbol{n}\, dS_K + \int_K \Phi_i \boldsymbol{S}(\boldsymbol{U}_h)\, dK$$

- Use the LLF or Roe's flux to evaluate the interface fluxes

LLF

$$\widehat{\boldsymbol{Q}}(\boldsymbol{U}_h) = 0.5 \left[\boldsymbol{Q}^{+}(\boldsymbol{U}_h) \cdot \boldsymbol{n} + \boldsymbol{Q}^{-}(\boldsymbol{U}_h) \cdot \boldsymbol{n} - \lambda_{\max} (\boldsymbol{U}_h^{-} - \boldsymbol{U}_h^{+}) \right]$$

DG discretization of the viscous terms

ERAU

- Define the auxiliary variable $\Theta = \nabla \mathbf{U}_f$ for the gradient of the state vector and discretize it in the same DG framework

$$\mathbf{M}\boldsymbol{c} = \int_{S_K} \Phi_i \overset{\downarrow}{\boldsymbol{U}}_h \cdot \boldsymbol{n} dS_K - \int_K \nabla \Phi_i \cdot \boldsymbol{U}_h dK$$

- Use the LDG or the BR2 scheme to evaluate the numerical fluxes
- For the computations we used the LDG method
- For arbitrary three dimensional meshes the BR2 scheme is more suitable because it yields more narrow stencils strictly confined to the immediate neighbors of an element

TVB limiting for the flow field variables

ERAU

- To eliminate oscillations at strong discontinuities of both the flow field and the electromagnetic field variable the following TVB limiter is used

$$\bar{m}(a_1, a_2, a_3) = \begin{cases} a_1 & \text{if } |a_1| \le \wp L^2 \\ m(a_1, a_2, a_3) & \text{otherwise} \end{cases}$$

the parameter $\wp$ is an estimation of second order derivative of variable u and it is estimated by the Laplacian $\wp(u)$; $\nabla^2 u$ in the transformed space

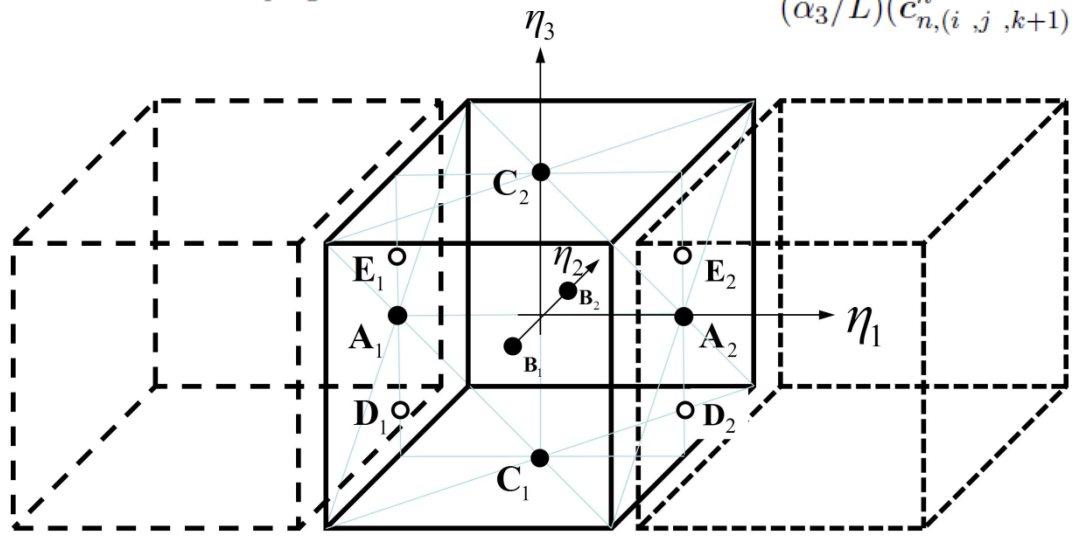
- The TVB limiter is applied to the characteristic variables of the flow field
- Limiting is performed in the transformed canonical space of cubic elements and the limited variables are transferred back to the physical domain using collapsed coordinates
- Limiting is applied to all variable at the end of each RK stage

TVB limiting

Hierarchical Limiter

$$u_h^h = \sum_{i=0}^{26} c_i^h b_i^h$$

$$\begin{aligned}\widetilde{c_i^h} = m\big(c_i^h, &(\alpha_1/L)(c^h_{l,(i+1,j\ ,k)} - c^h_{l,(i\ ,j\ ,k)}\ \ ), (\alpha_1/L)(c^h_{l,(i\ ,j\ ,k)} - c^h_{l,(i-1,j\ ,k)}),\\ &(\alpha_2/L)(c^h_{m,(i\ ,j+1,k)} - c^h_{m,(i\ ,j\ ,k)}), (\alpha_2/L)(c^h_{m,(i\ ,j\ ,k)} - c^h_{m,(i\ ,j-1,k)}),\\ &(\alpha_3/L)(c^h_{n,(i\ ,j\ ,k+1)} - c^h_{n,(i,j\ ,k)}\ \ ), (\alpha_3/L)(c^h_{n,(i\ ,j\ ,k)} - c^h_{n,(i-1,j\ ,k-1)})\big)\end{aligned}$$



element $(i-1)$ *element* (i) *element* $(i+1)$

P1 Limiter

$$\overline{m}(a_1, a_2, \ldots, a_n) = \begin{cases} a_1 & \text{if } |a_1| \le ML_{x,y,z}^2 + b, \\ m(a_1, a_2, \ldots, a_n) & \text{otherwise.} \end{cases}$$

$$\begin{aligned}u_h^h = c_0^h + c_1^h\eta_1 \quad &+ c_2^h\eta_2 \quad + c_3^h\eta_3\\ &+ c_4^h\eta_1\eta_2 + c_5^h\eta_1\eta_3 + c_6^h\eta_2\eta_3\\ &+ c_7^h\eta_1\eta_2\eta_3\end{aligned}$$

$$U_{A_1} = u^h(-1,0,0) - c_0^h = -c_1^h,$$

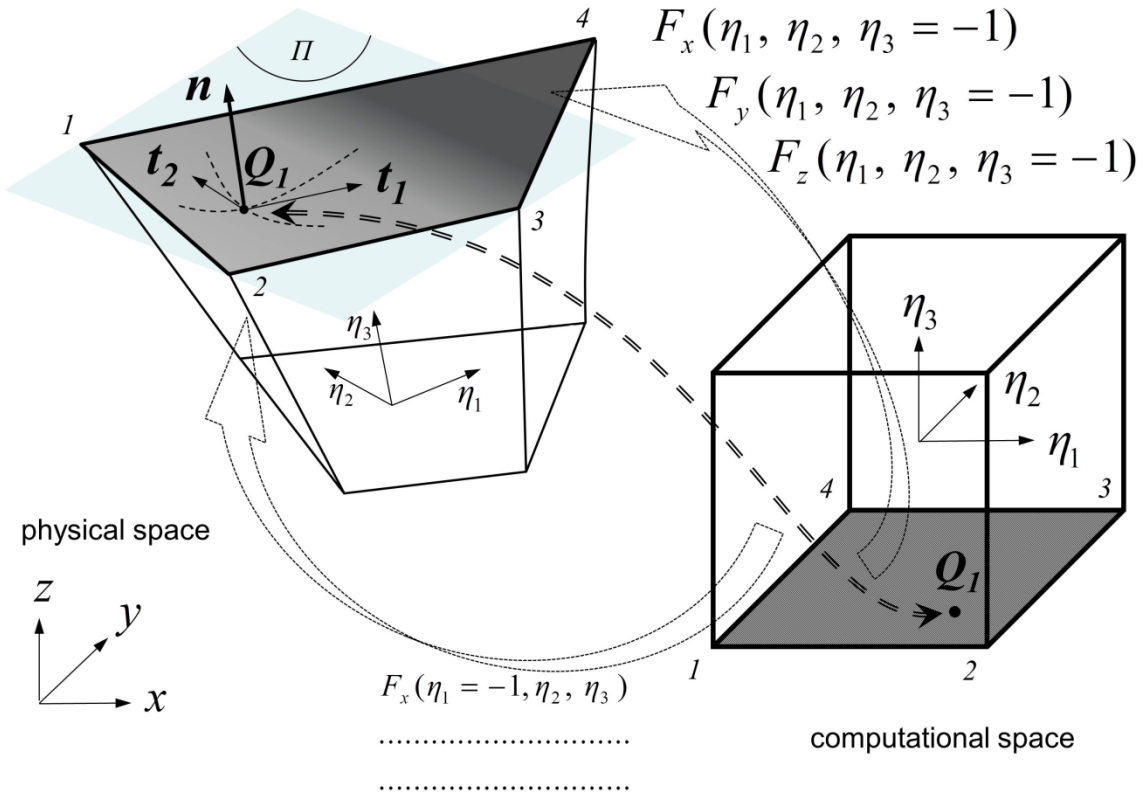
$$U_{A_2} = u^h(1,0,0) - c_0^h = c_1^h,$$

$$\widetilde{U}_{A_1} = -m(-U_{A_1}, c^h_{0,(i+1,j,k)} - c^h_{0,(i,j,k)}, c^h_{0,(i,j.k)} - c^h_{0,(i-1,j,k)}),$$

$$\widetilde{U}_{A_2} = m(U_{A_2}, c^h_{0,(i+1,j,k)} - c^h_{0,(i,j,k)}, c^h_{0,(i,j,k)} - c^h_{0,(i-1,j,k)}),$$

$$\widetilde{c_1^h} = \frac{\widetilde{U}_{A_2} - \widetilde{U}_{A_1}}{2}.$$

Non-planar face treatment for meshes with warped elements



$$n = \frac{t_1 \times t_2}{|t_1 \times t_2|}$$

$$t_1 = \left(\frac{dx}{d\eta_i}, \frac{dy}{d\eta_i}, \frac{dz}{d\eta_i}\right), t_2 = \left(\frac{dx}{d\eta_j}, \frac{dy}{d\eta_j}, \frac{dz}{d\eta_j}\right)$$

$u_1 = 8.25$

$\rho_1 = 5.7$

$p_1 = 116.5$

$a_1 = 5.35$

$W = 10a_1$

$u_p = 8.25a_1$



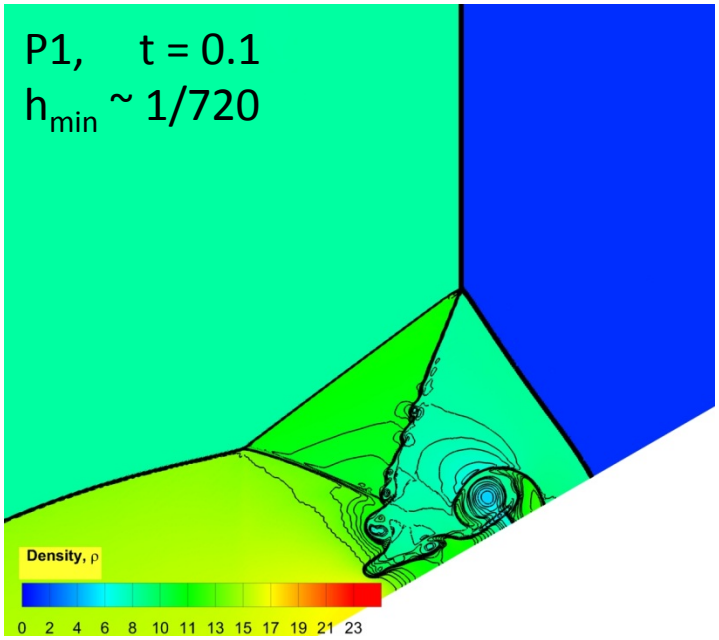
$u_2 = 0$

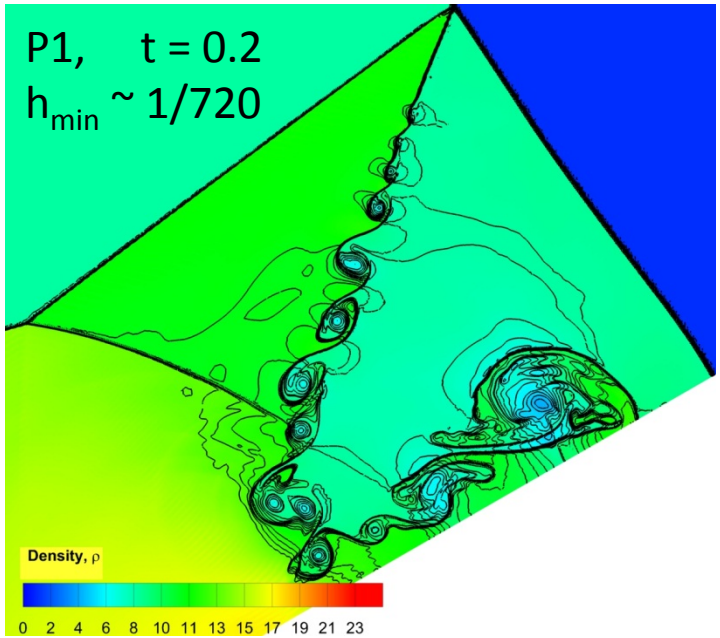
$\rho_2 = 1$

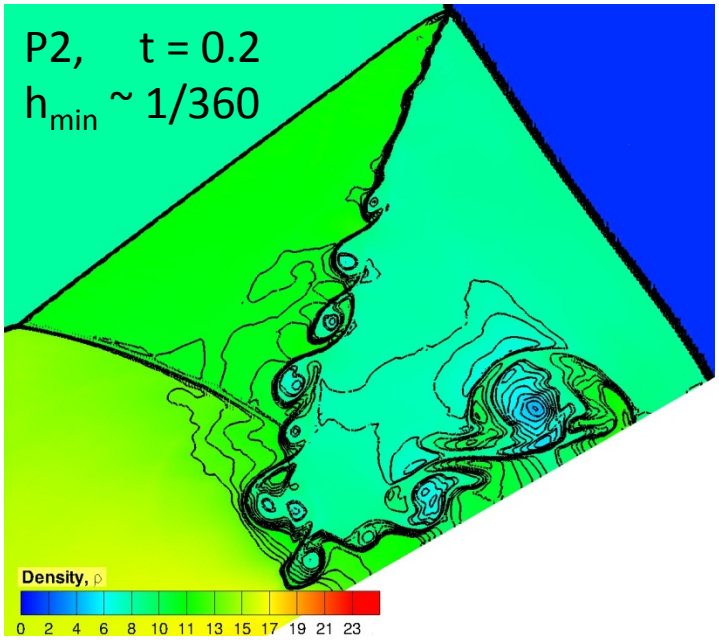
$p_2 = 1$

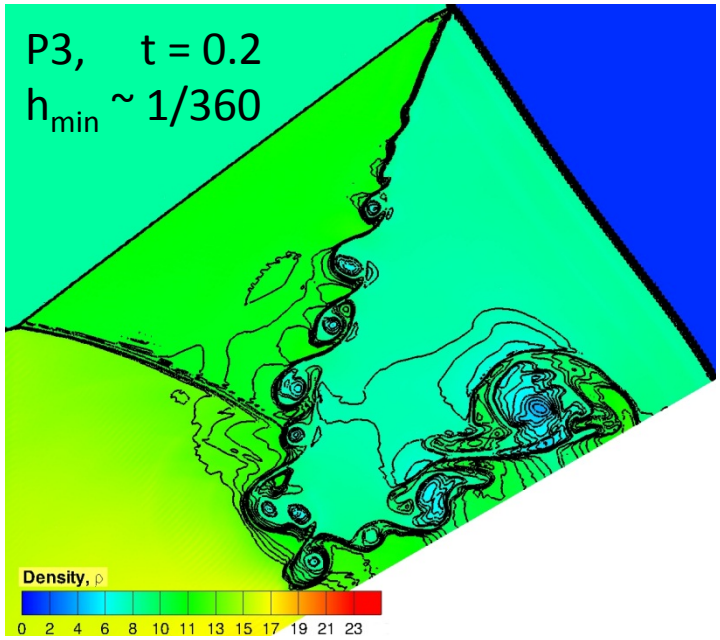
$a_2 = \sqrt{\gamma}$

Double Mach reflection of a M = 10 moving shock





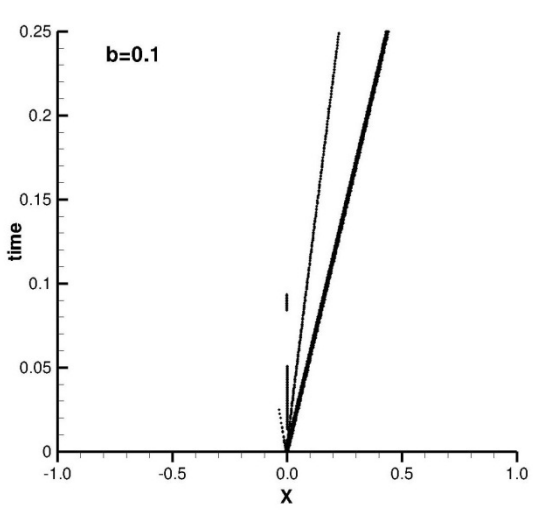


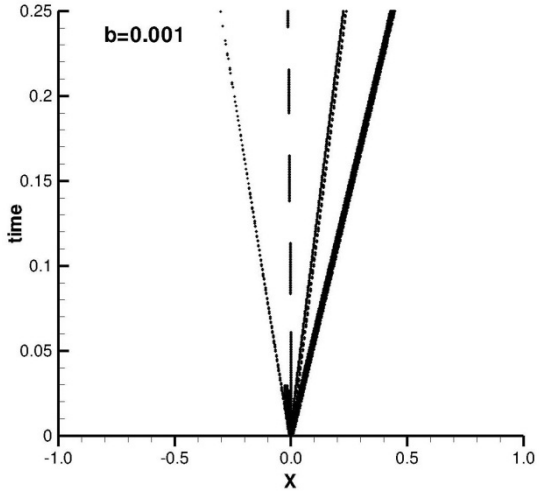


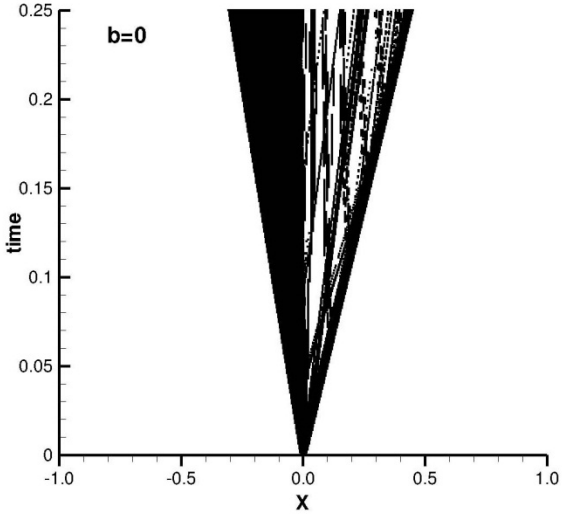
Sod's shock tube problem

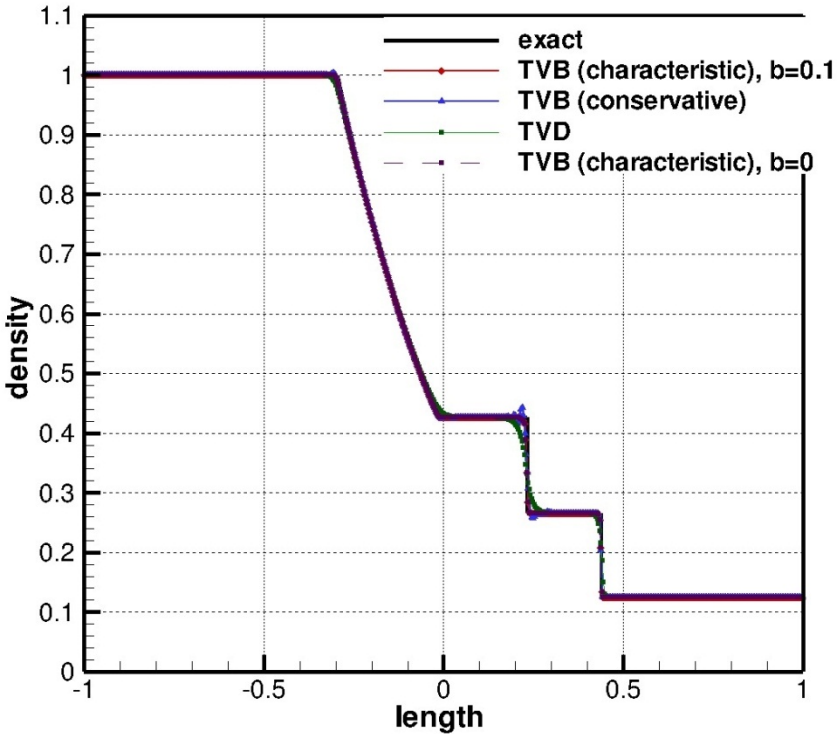
$[\rho_L,\ u_L, p_L]$
$[1.0, 0.0, 1.0]$

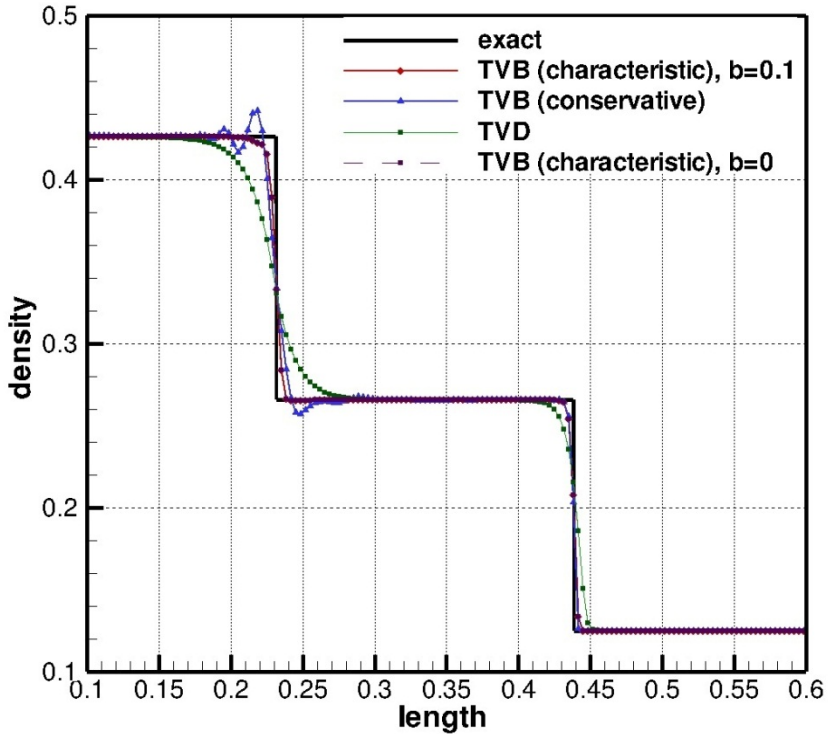
$[\ \rho_R,\ \ u_R, p_R]$
$[0.125, 0.0, 0.1]$







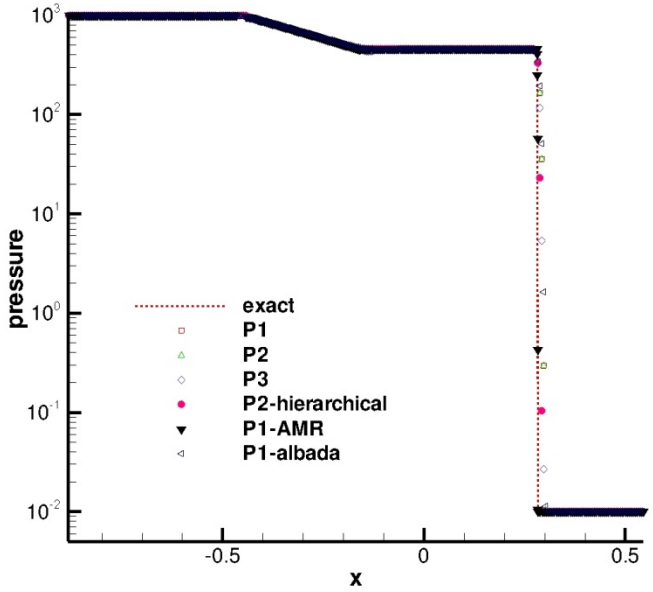




High pressure ratio shock tube problem

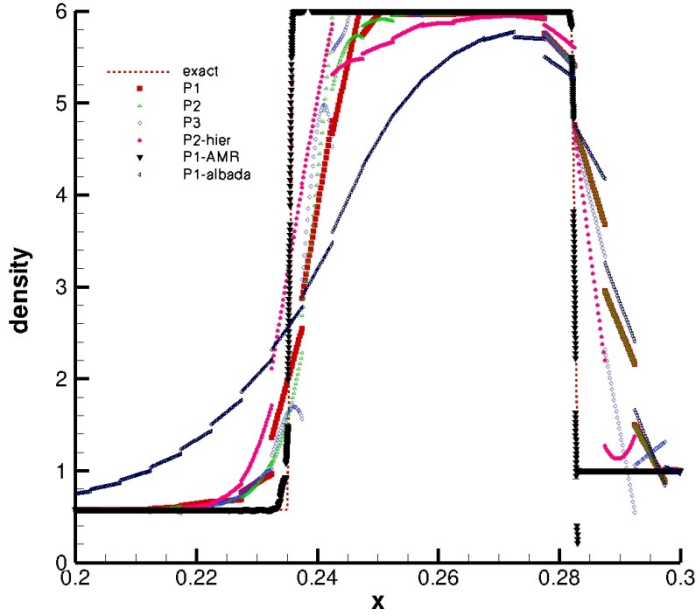
$[\rho_L,\ u_L,\ \ p_L]$
$[1.0, 0.0, 1000.0]$

$[\rho_R,\ u_R,\ p_R]$
$[1.0, 0.0, 0.01]$



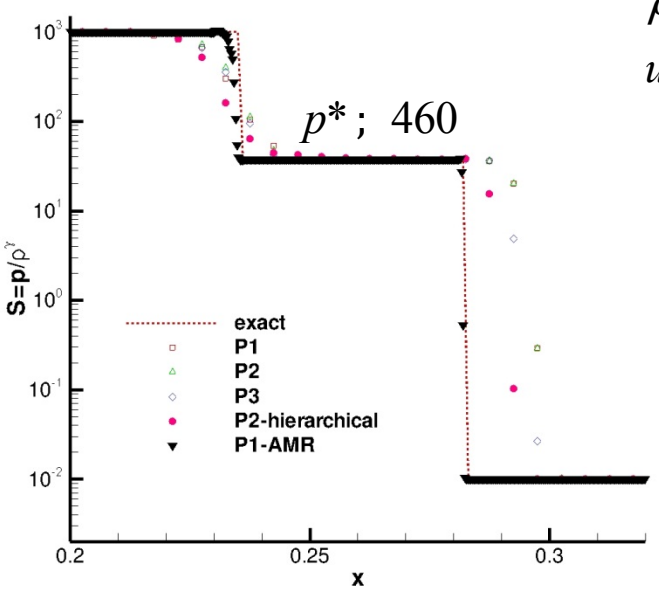
$p_L^{shock} / p_R^{shock}$; 46000

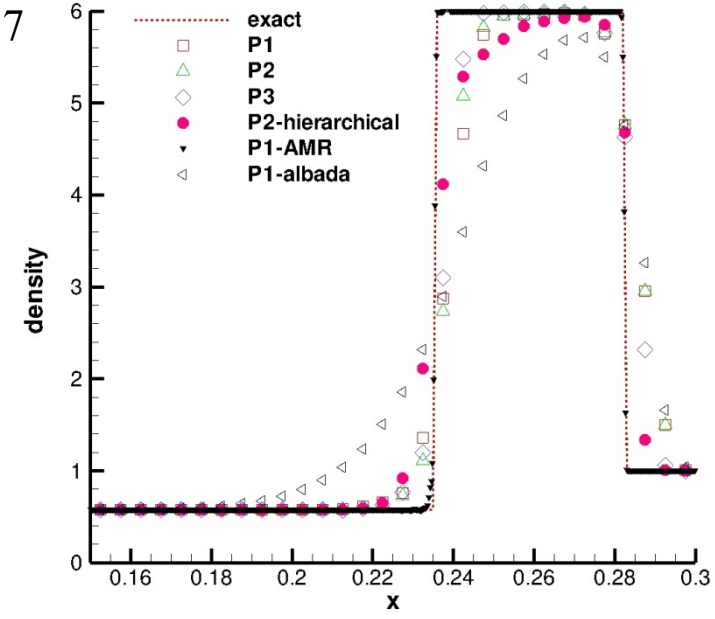
M_{shock} ; 198



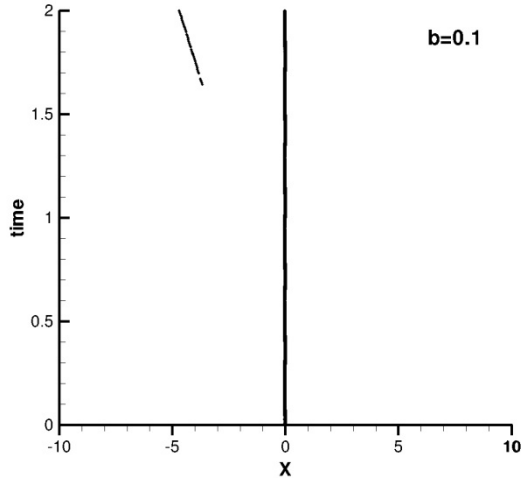
$\rho_L^{contact} / \rho_R^{contact}$; 5.99 / 0.57

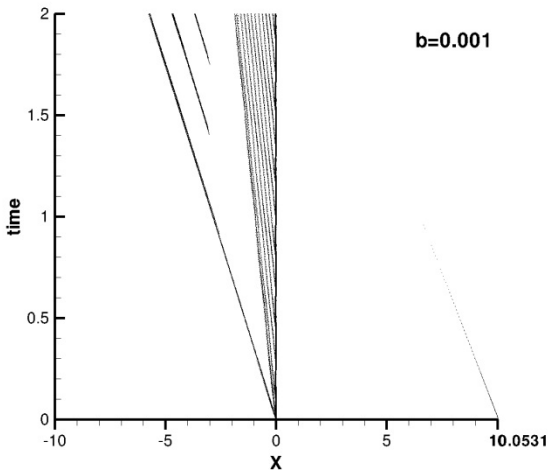
u_c ; 19.59

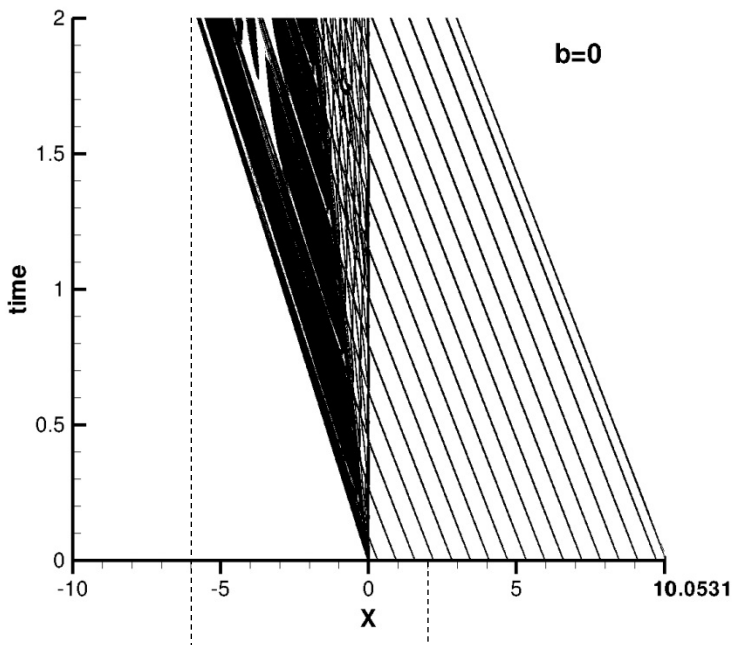


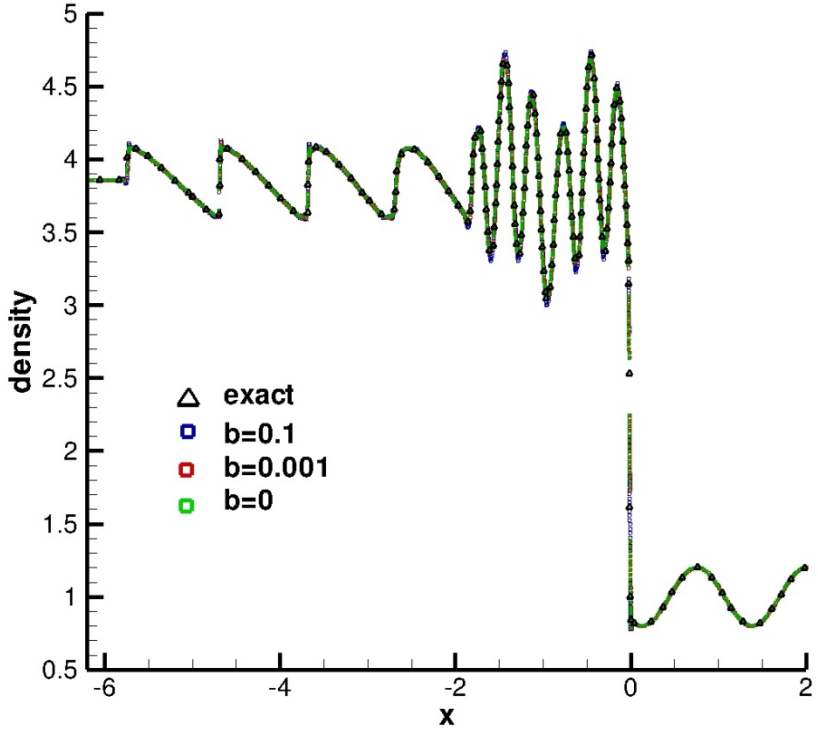


Shu & Osher problem M=3 shock-entropy interaction





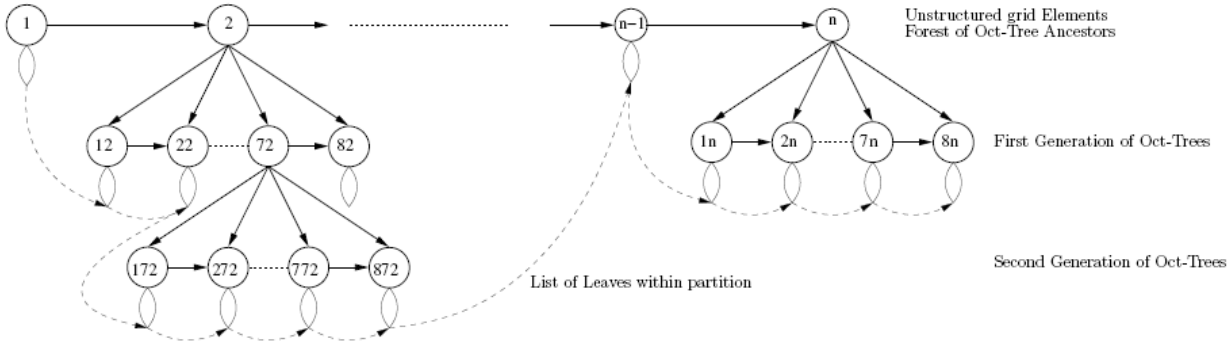




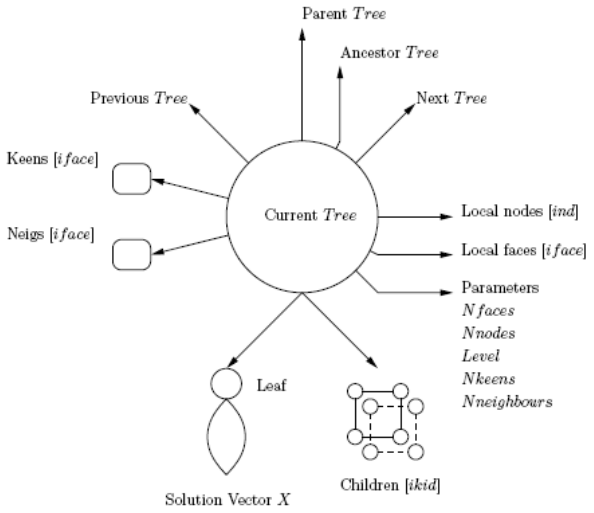
$$(\rho, u, p) = \begin{cases} 3.857143, -0.920279, 10.33333 & \text{if } -10 \leq x \leq 0 \\ 1 + 0.2sin(5x), -3.549648, 1.0 & \text{if } 0 < x \leq 10.0530964 \\ 1.0, -3.549648, 1.0 & \text{if } x > 10.0530964 \end{cases}$$

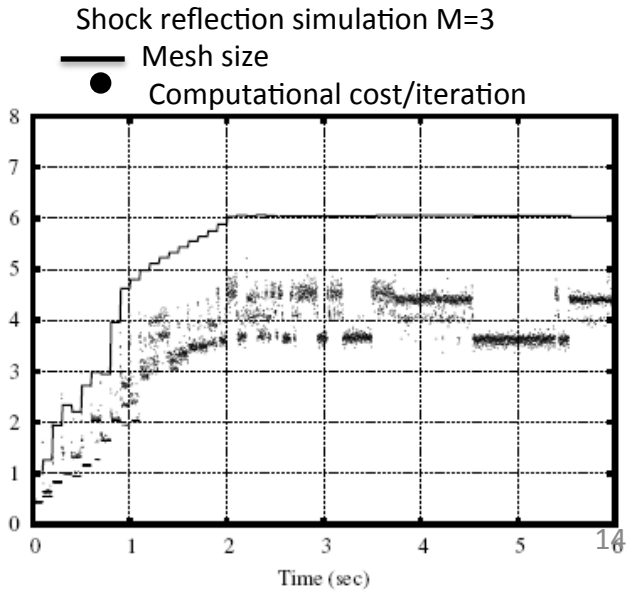
H-adaptivity for hybrid meshes

- The mesh is represented as linked list of oct-Trees creating a forest.



- Each tree is connected to it's accentors, to the next tree in the global list, to the next tree in the local list within the partition, to it's physical neighbors and to either it's children or to the actual element i.e. the leaf.
- The forest structure allows refining and coarsening on demand during the solution On the fly repartitioning of the adapted mesh, Arbitrary number of adaptation levels Explicit calculation of the connectivity and orientation of the faces.

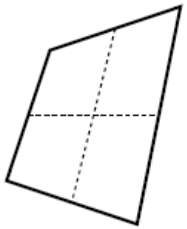


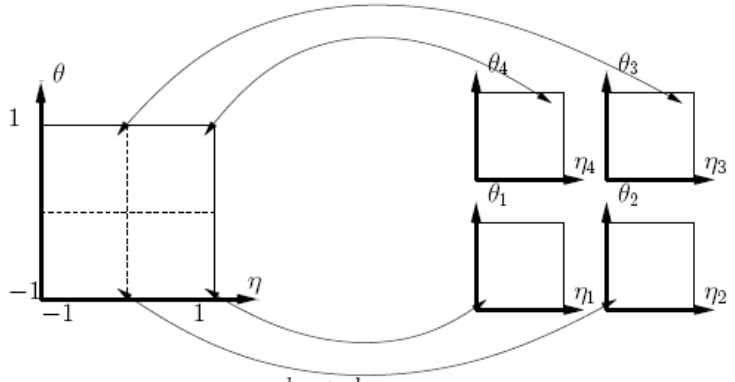


H-adaptivity for hybrid meshes

- The calculation of the fluxes on the faces and the accurate projection of the solution within the volume during merging or splitting is achieved by using the transformations from the computational to the physical space.

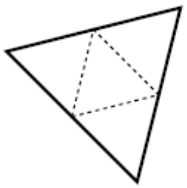
Hexahedral elements

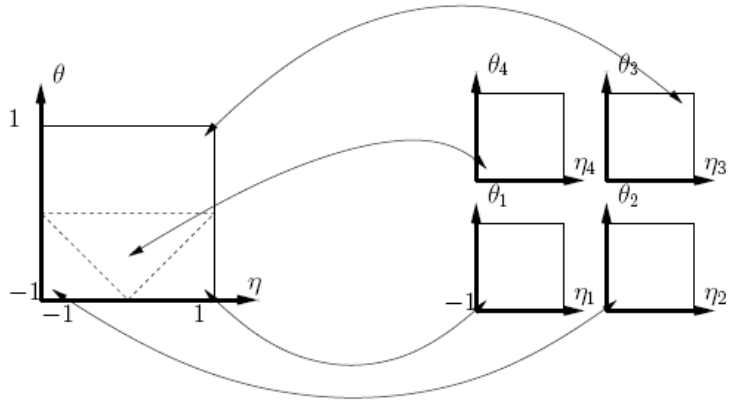




$$\eta = b\eta_i + d$$
$$\theta = f\theta_i + h$$

Prismatic elements

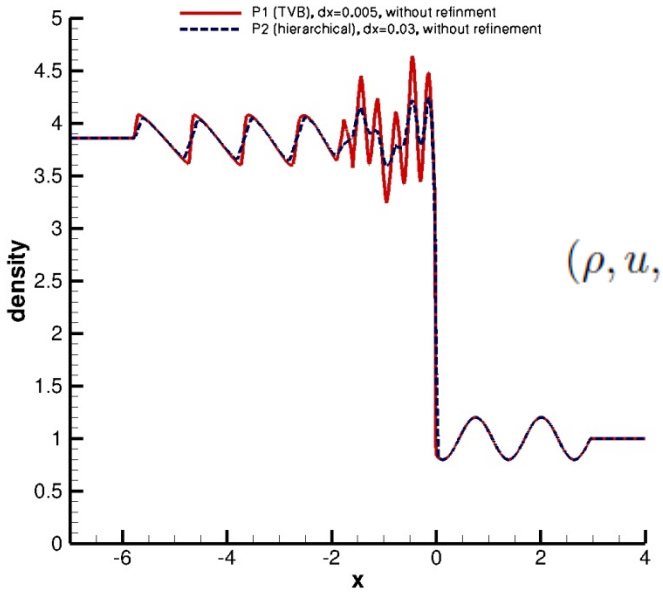




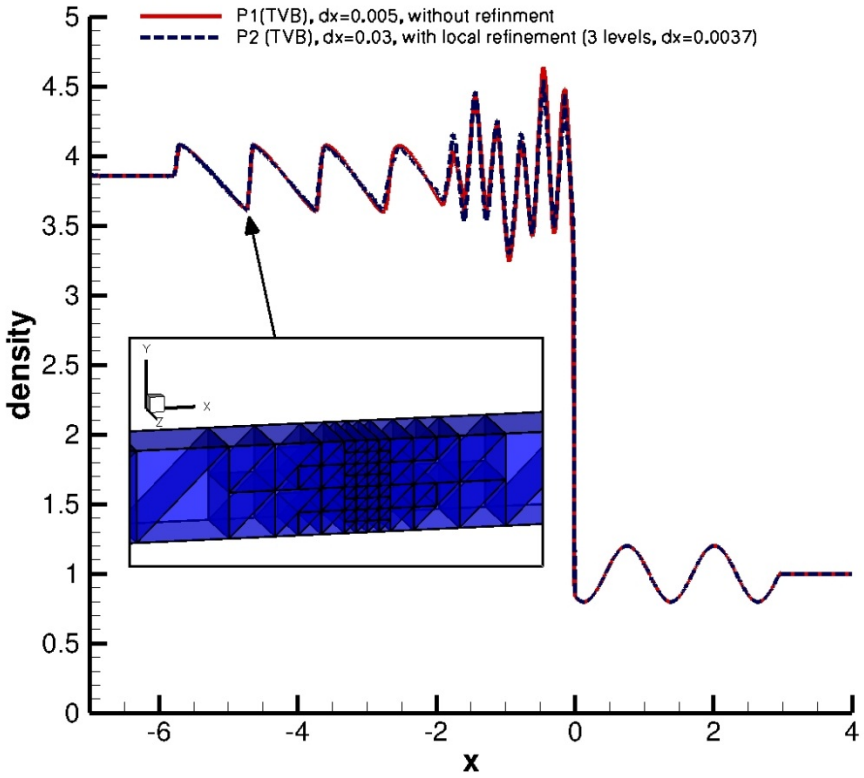
$$\eta = a\eta_i\theta_i + b\eta_i + c\theta_i + d$$
$$\theta = f\theta_i + h$$

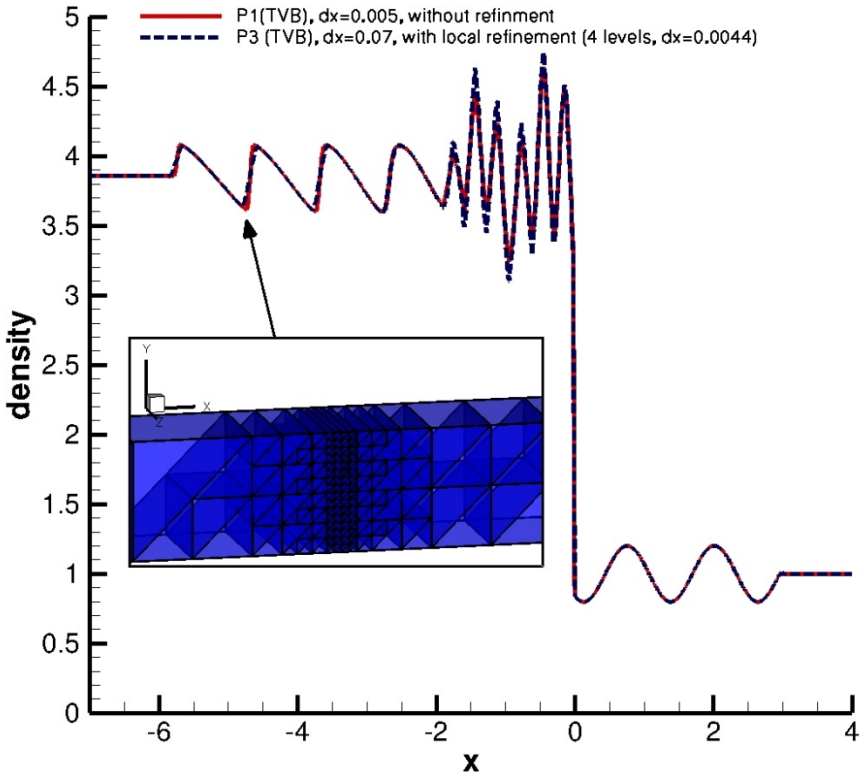
- The transformations are linear for hexahedral elements and second order in only one direction for prisms thus enabling the analytical solution of the reverse mapping of the quadrature points.

Effect of h/p refinement for the Shu & Osher M=3 shock-entropy interaction

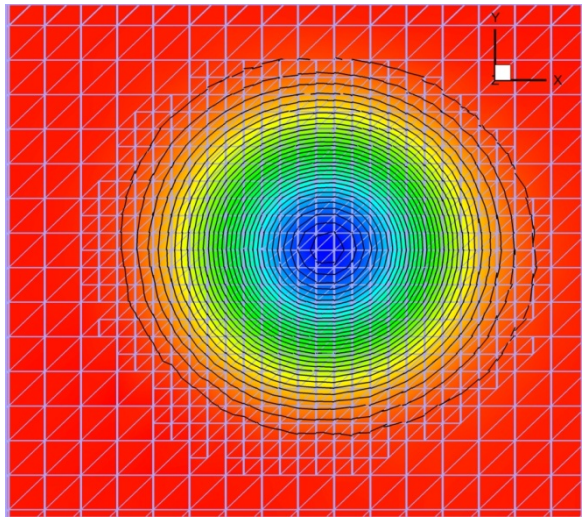


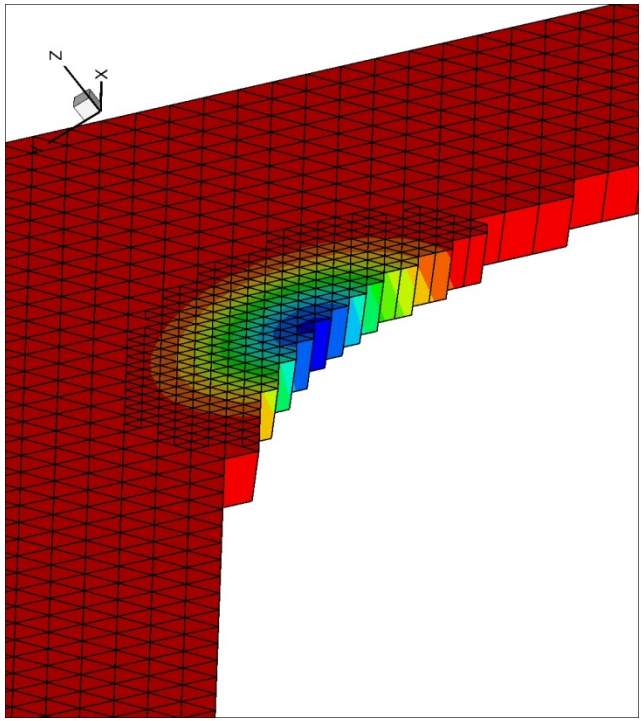
$$(\rho, u, p) = \begin{cases} 3.857143, -0.920279, 10.33333 & \text{if } -10 \leq x \leq 0 \\ 1 + 0.2sin(5x), -3.549648, 1.0 & \text{if } 0 < x \leq 10.0530964 \\ 1.0, -3.549648, 1.0 & \text{if } x > 10.0530964 \end{cases}$$





Convection of a 2D isentropic vortex in a 3D mesh

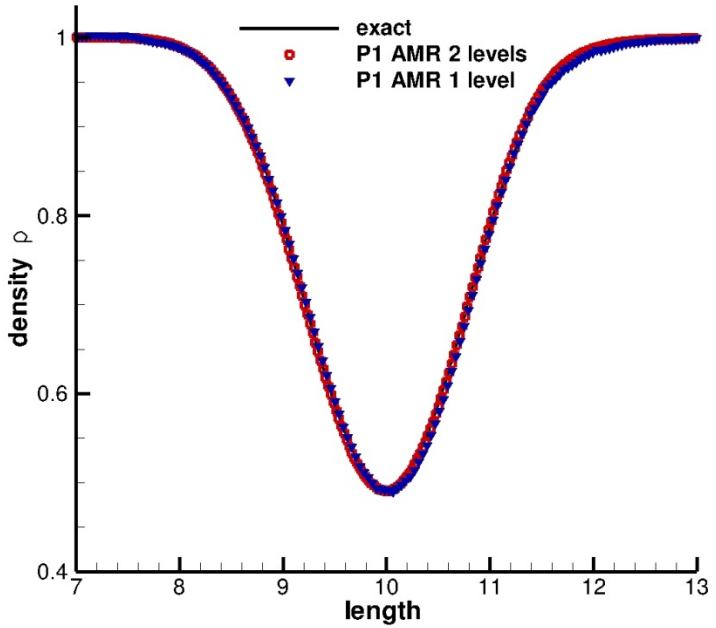


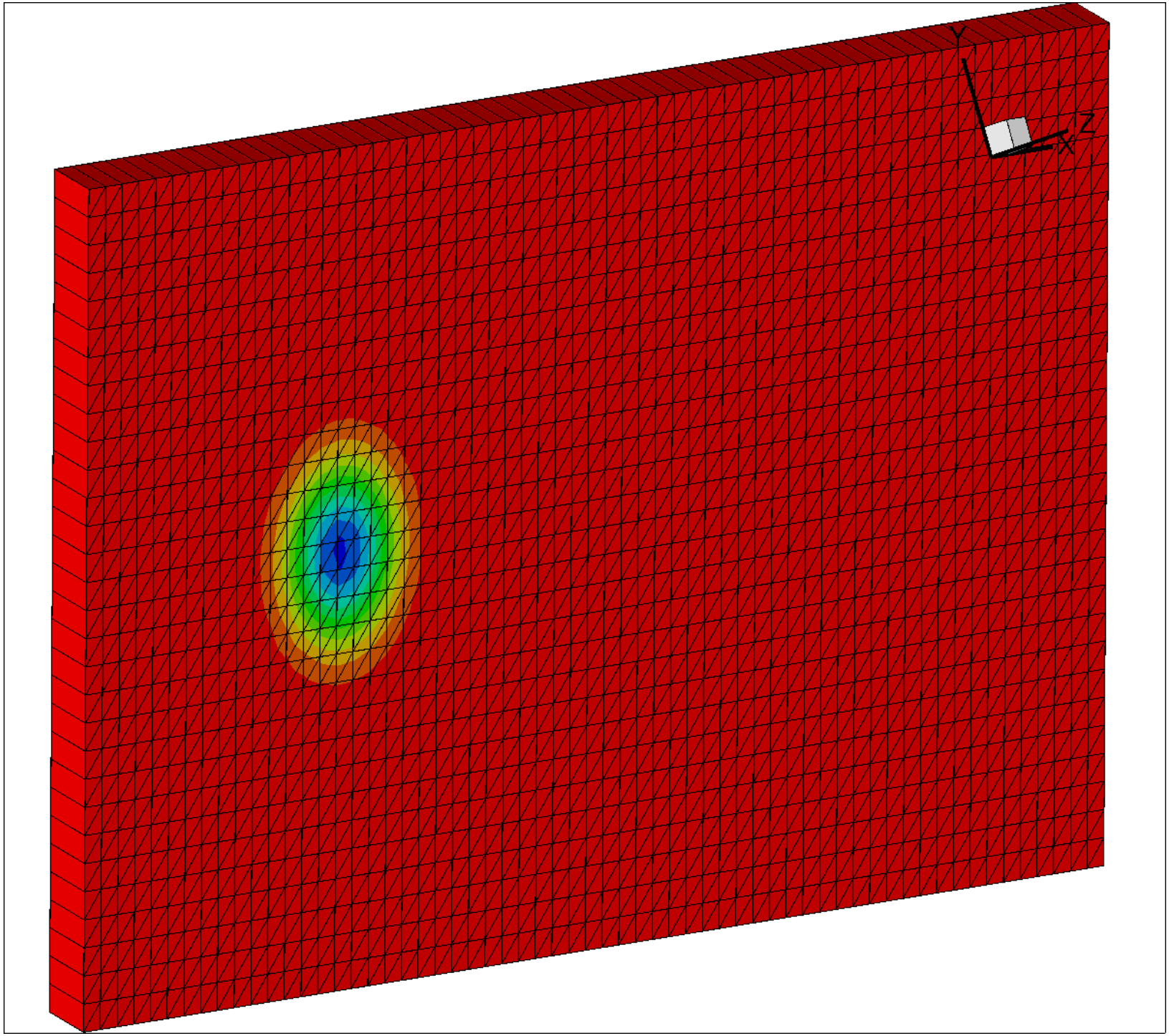


$$(\delta u, \delta v) = \frac{\beta}{2\pi}\exp(\frac{1-r^2}{2})[-y, x]$$

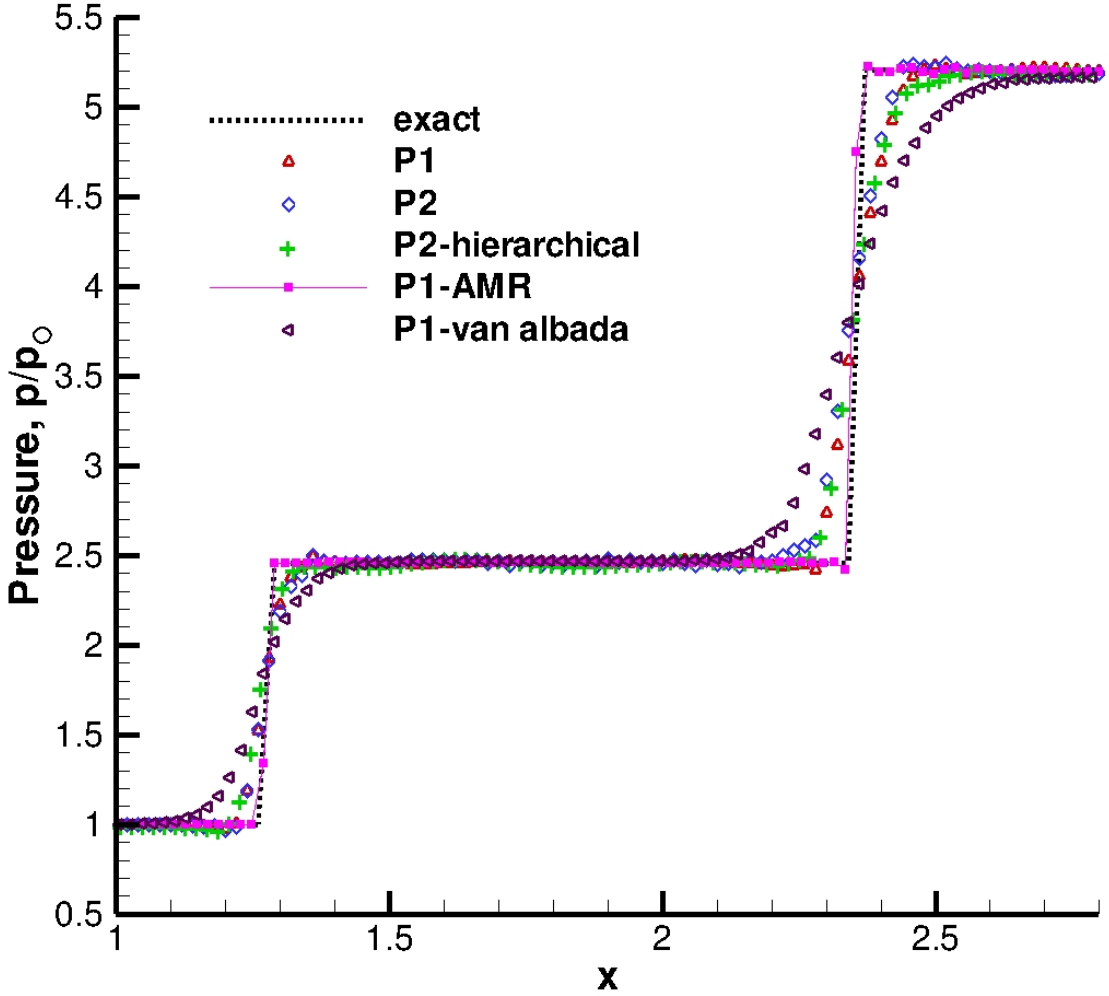
$$\delta\rho = [1 - \frac{(\gamma-1)\beta^2}{8\gamma\pi^2}\exp(1-r^2)]^{\frac{1}{\gamma-1}}, \quad p = \rho^{\gamma}/\gamma$$

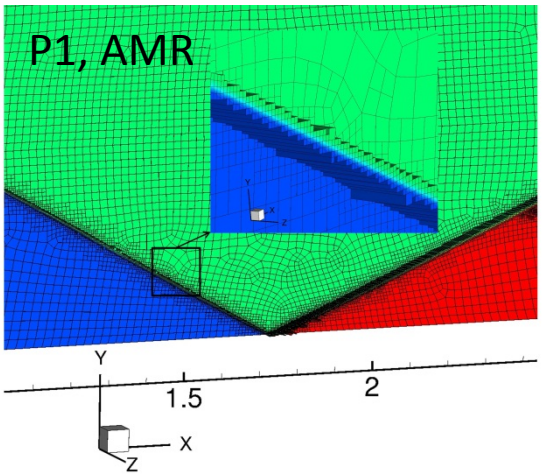
AMR level	L2 error	Convergence rate
1	1:52 x 10^{-2}	2.07
2	3.36 x 10^{-3}	2.07
3	8.05 x 10^{-4}	2.06

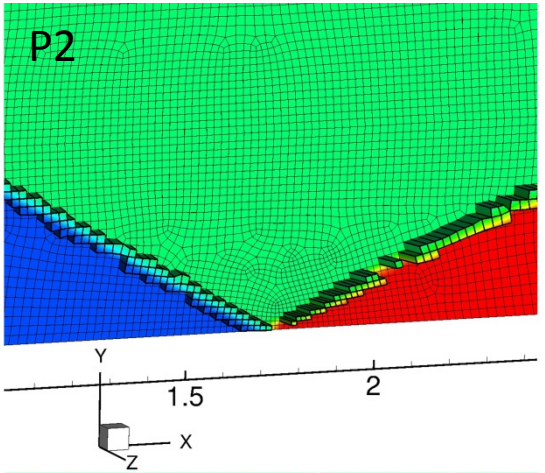


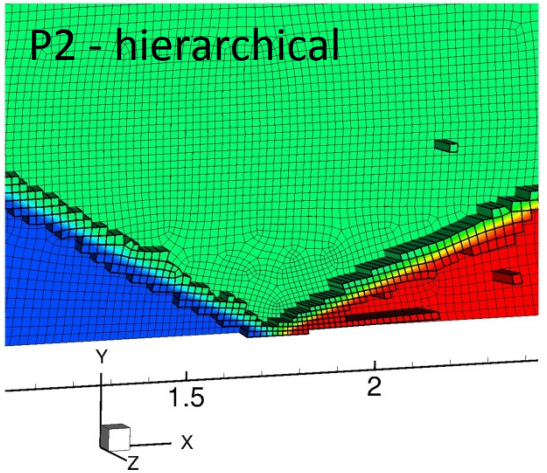

Y
Z
X

Oblique shock at M =3 and β=30o
Reflecting from a solid surface



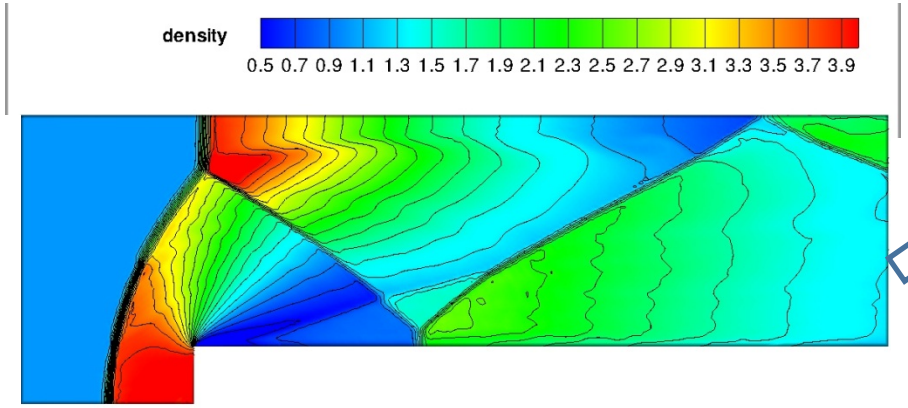


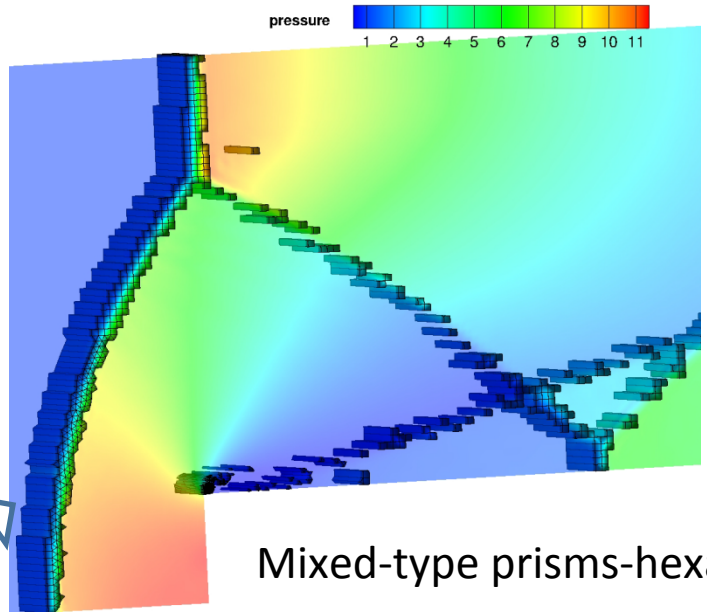




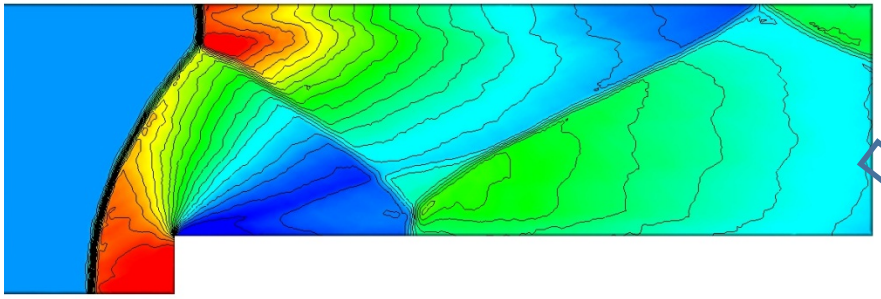
Flow in a tunnel with a step at M=3

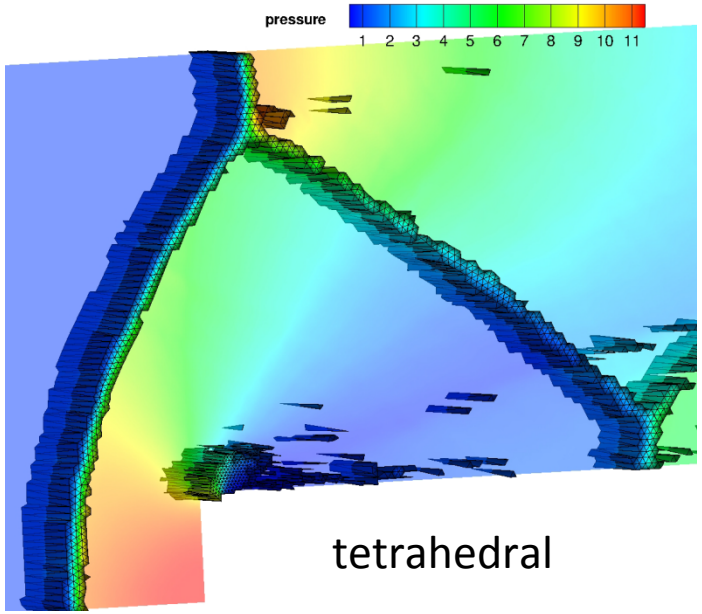
Computed density and pressure at t=4.0



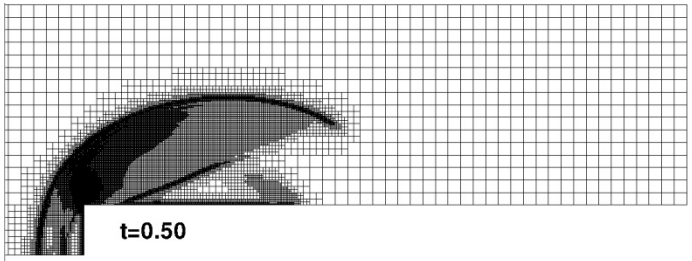


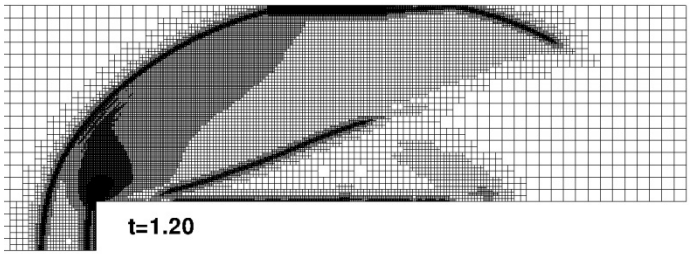
Mixed-type prisms-hexa





tetrahedral

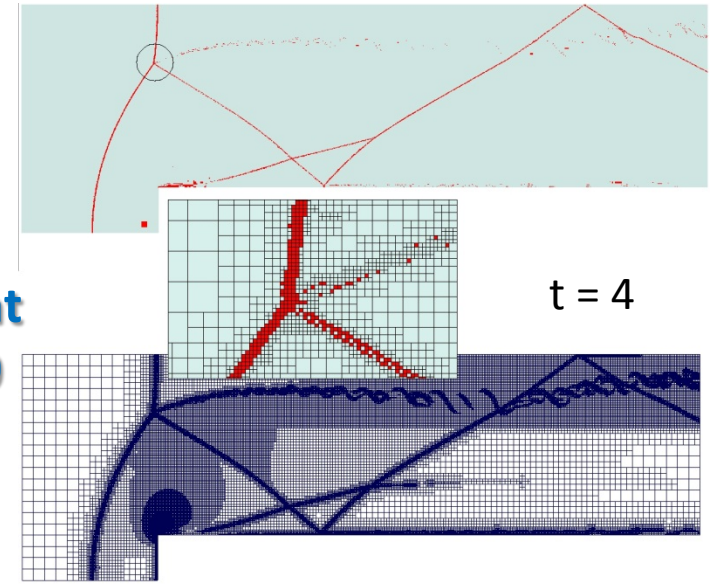


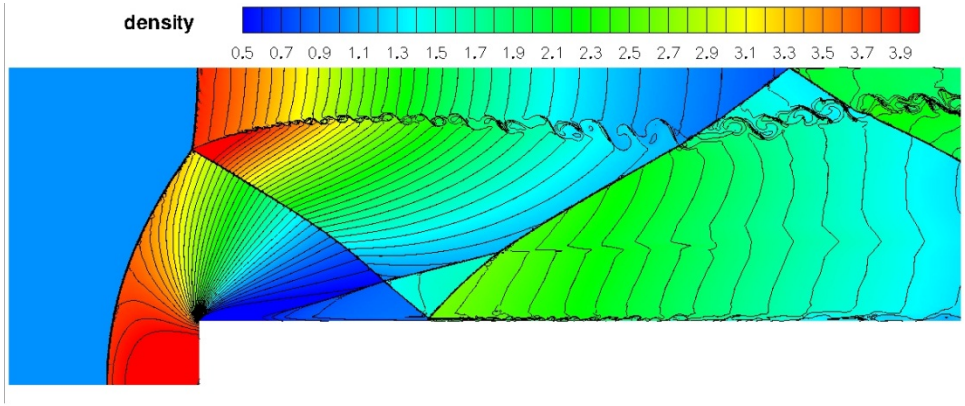


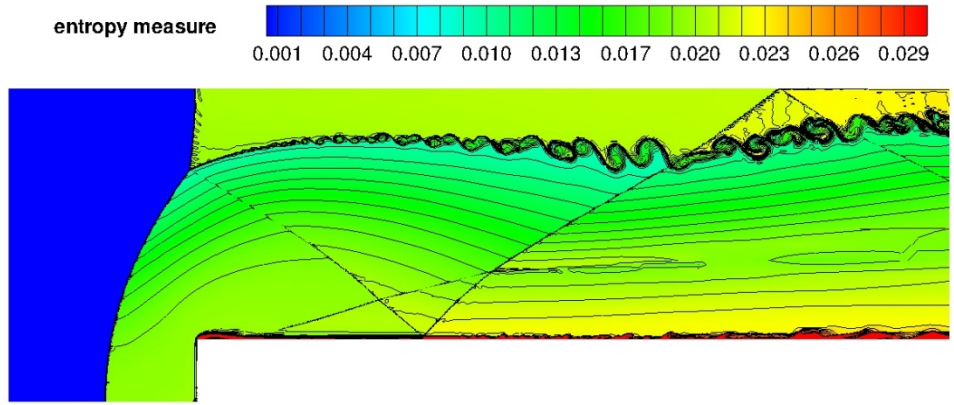
Dynamic AMR

5 levels of refinement

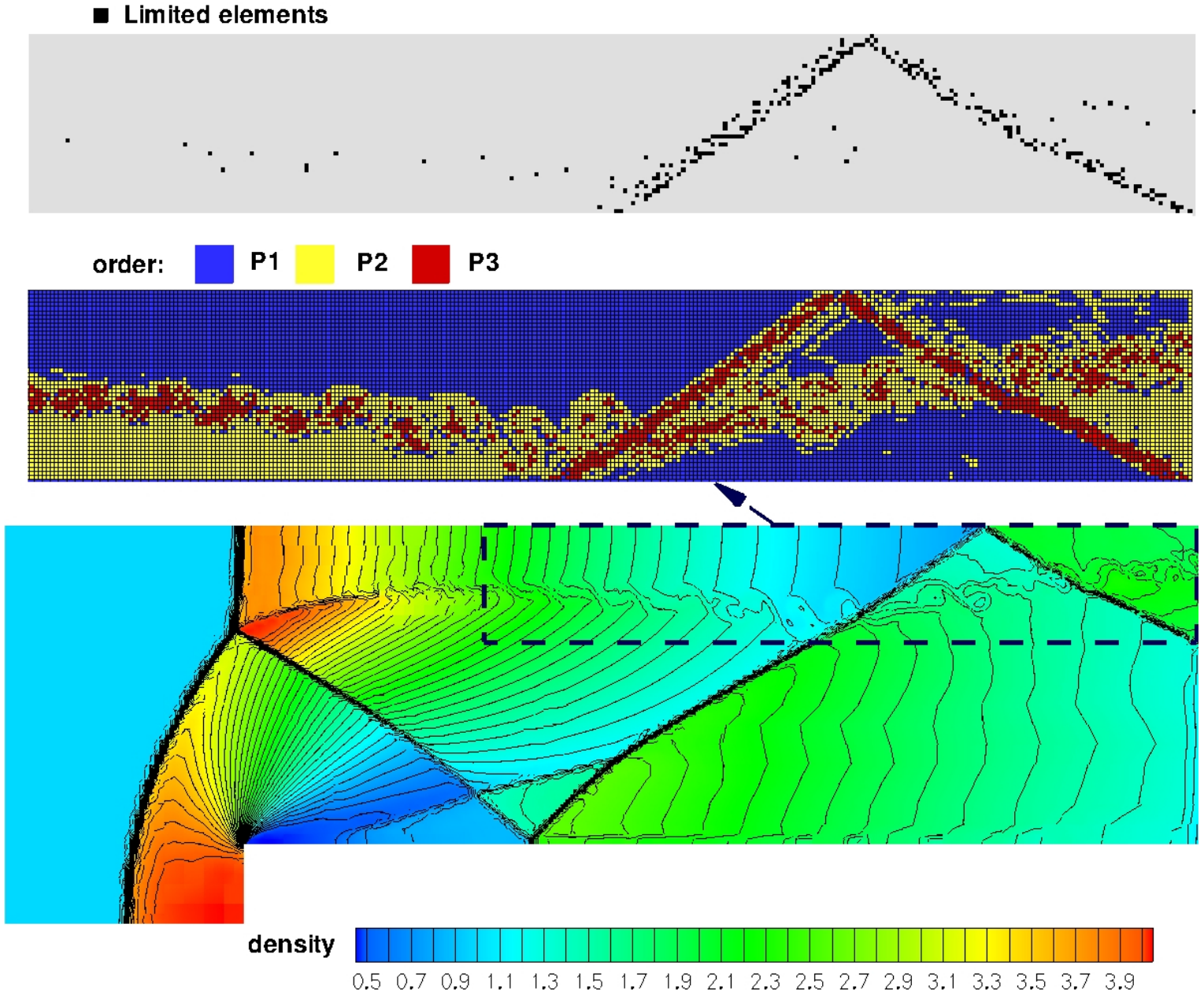
$h_{min} = 1/640$



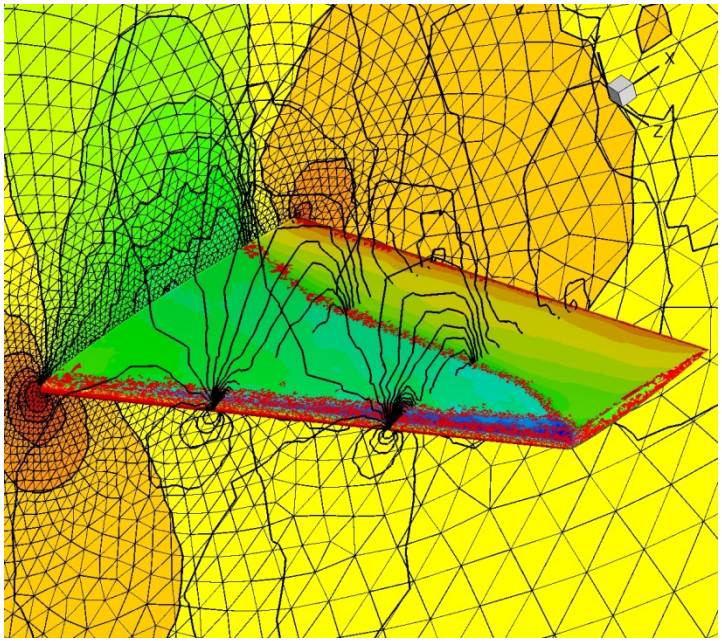


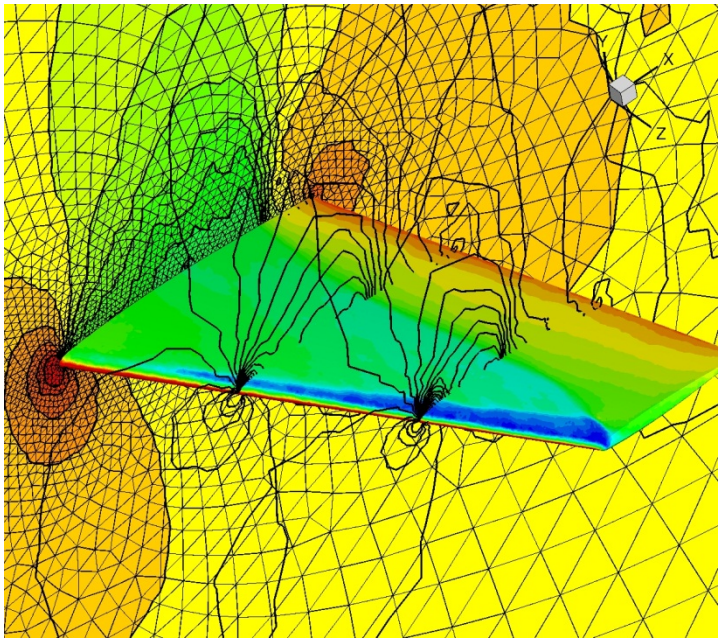


Combined dynamic AMR (4 levels, h_{min} = 1/320) and p-type refinement (P2, P3) for the roll-ups after the Mach stem (p-adaptation criterion is the computed vorticity)



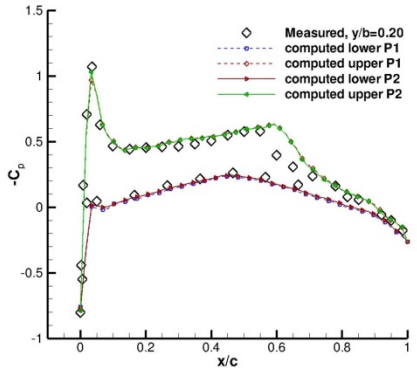
ONERA M6 wing at M = 0.84 and α = 3º



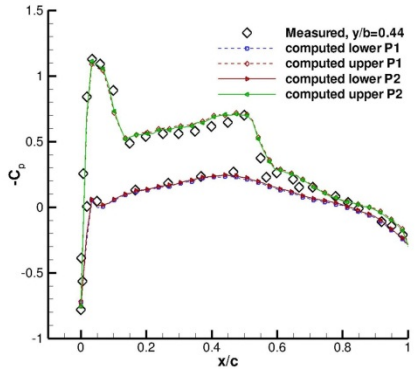


P1

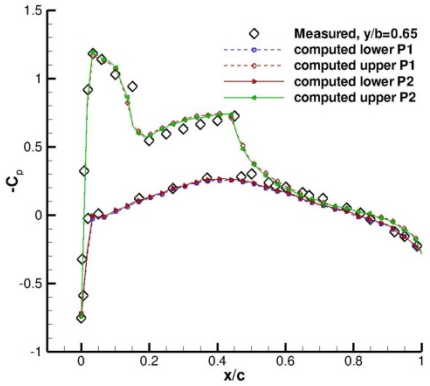
P2

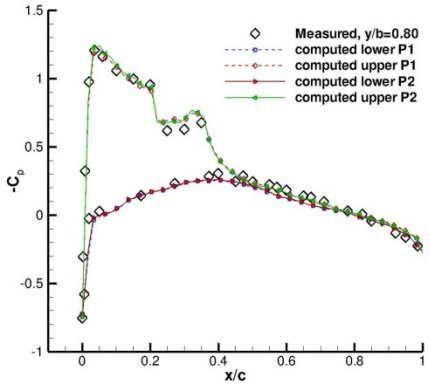


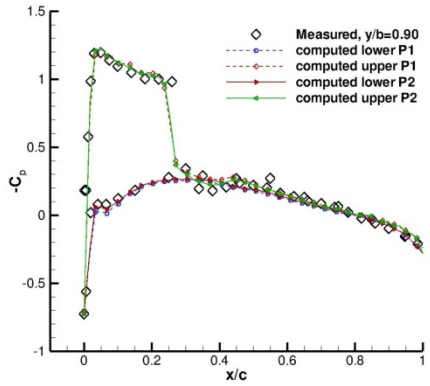
y/b = 0.20



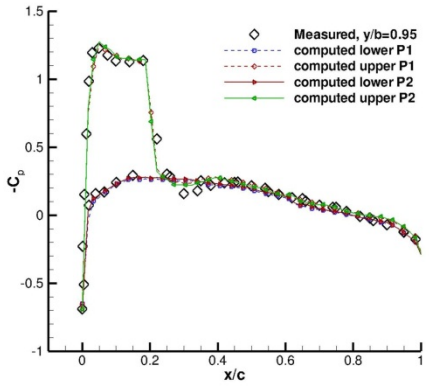
y/b = 0.44







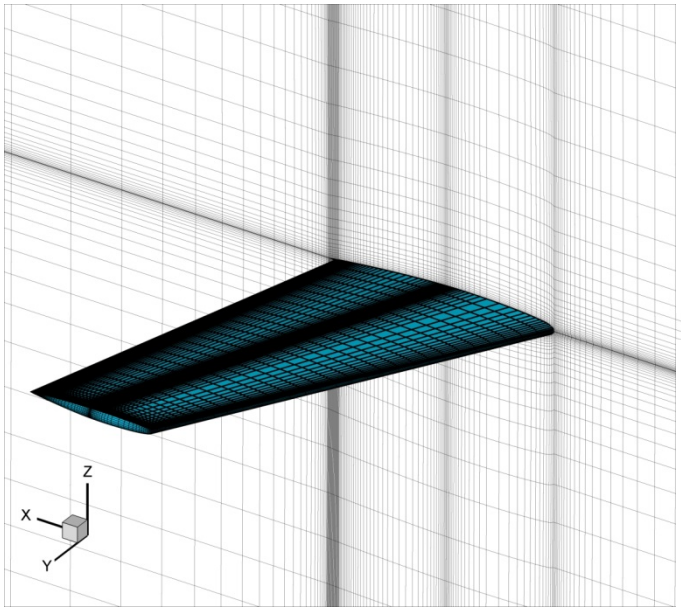
y/b = 0.90

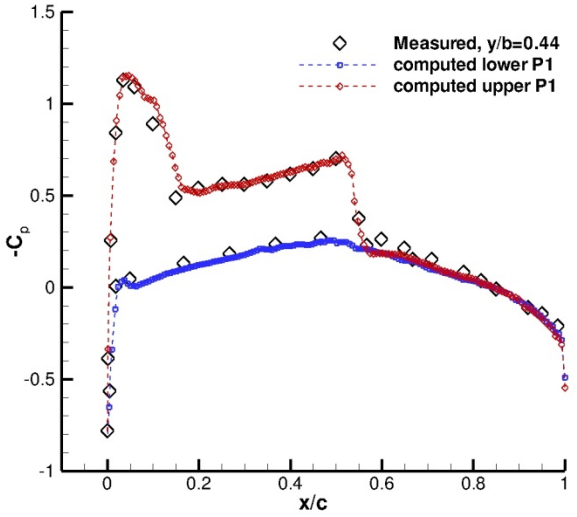


y/b = 0.95

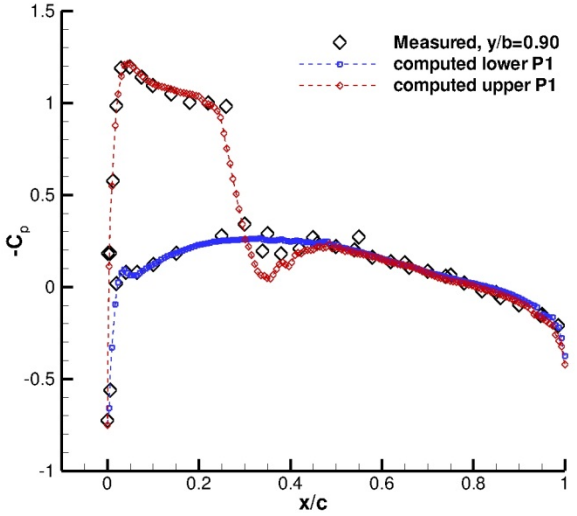
ONERA M6 wing at M = 0.84 and α = 3°

fine mesh, hexahedra with planar faces (no warping)

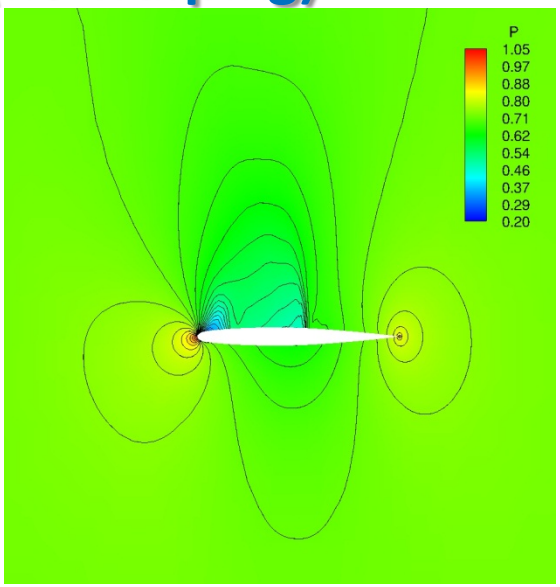


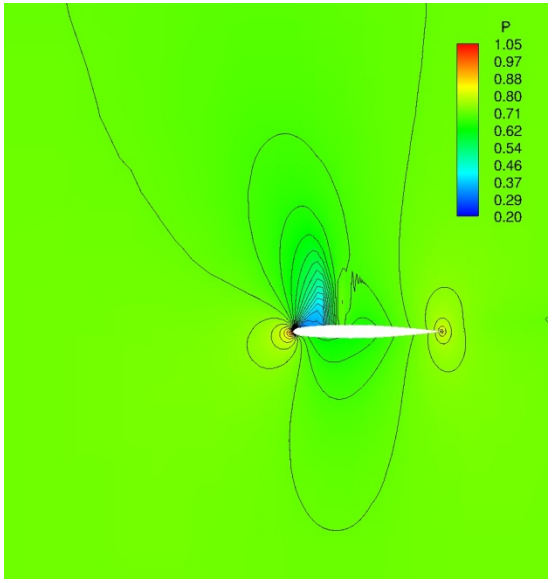


y/b = 0.44

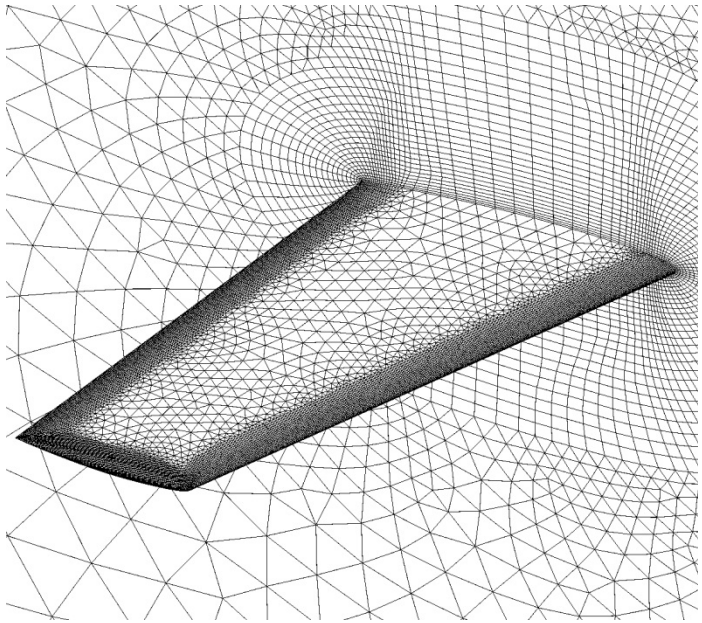


y/b = 0.9

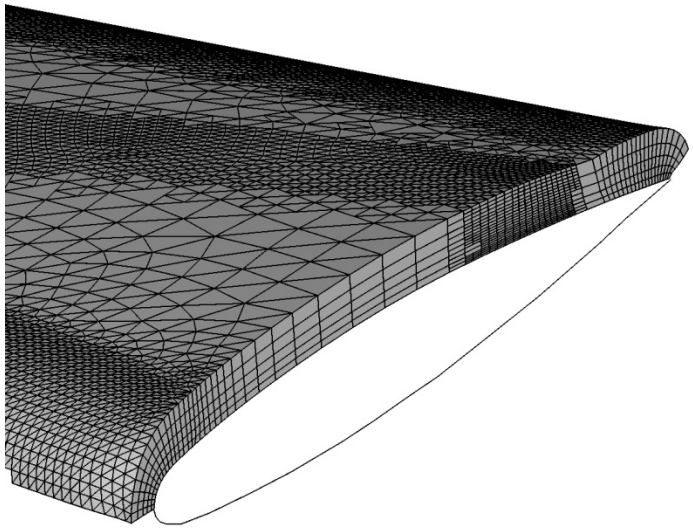




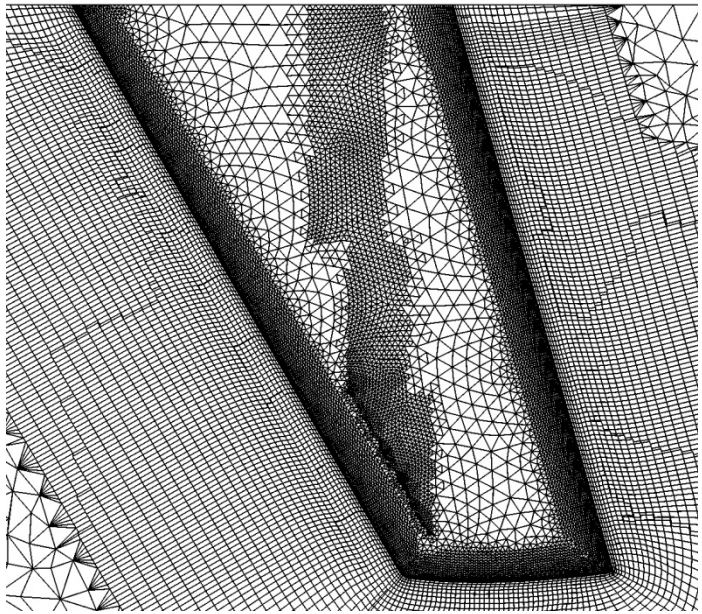
Initial surface mesh



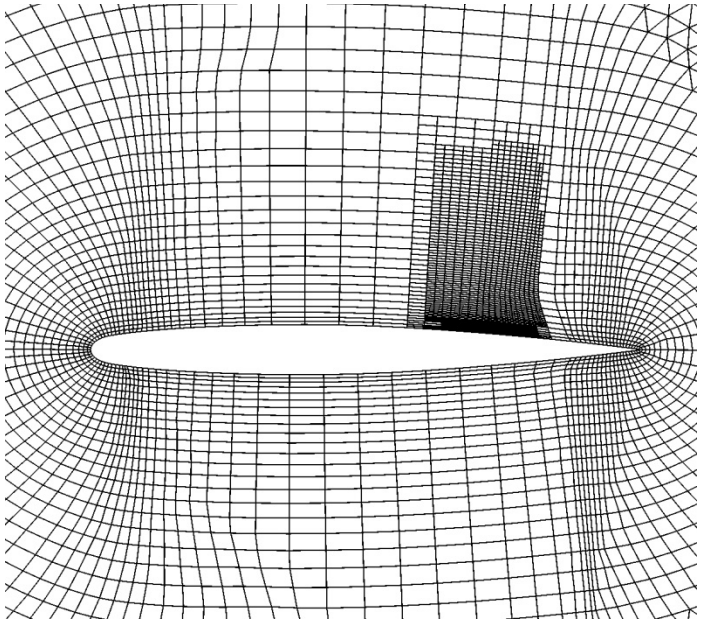
Near filed refined mesh



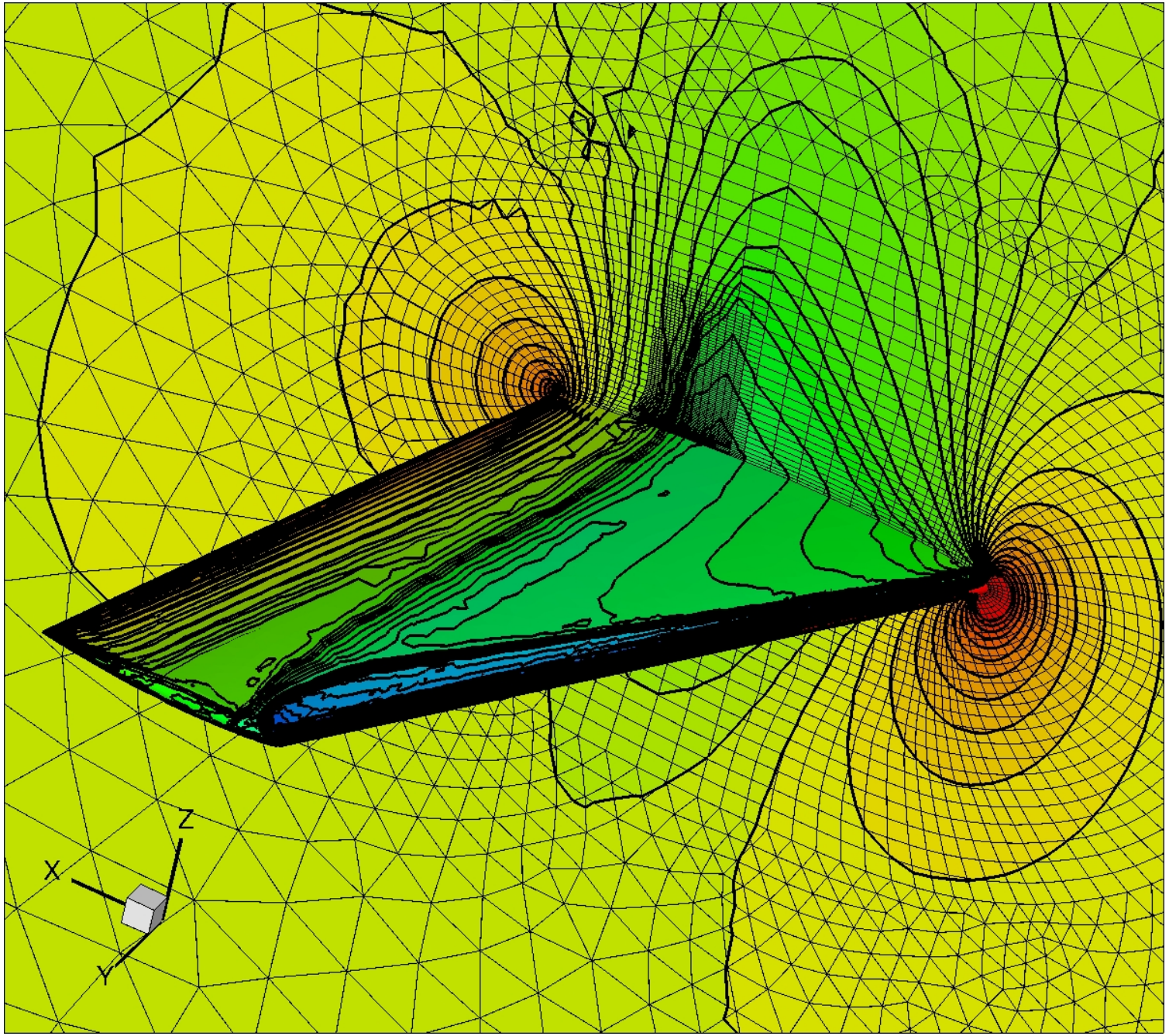
Surface mesh after 2 levels of AMR



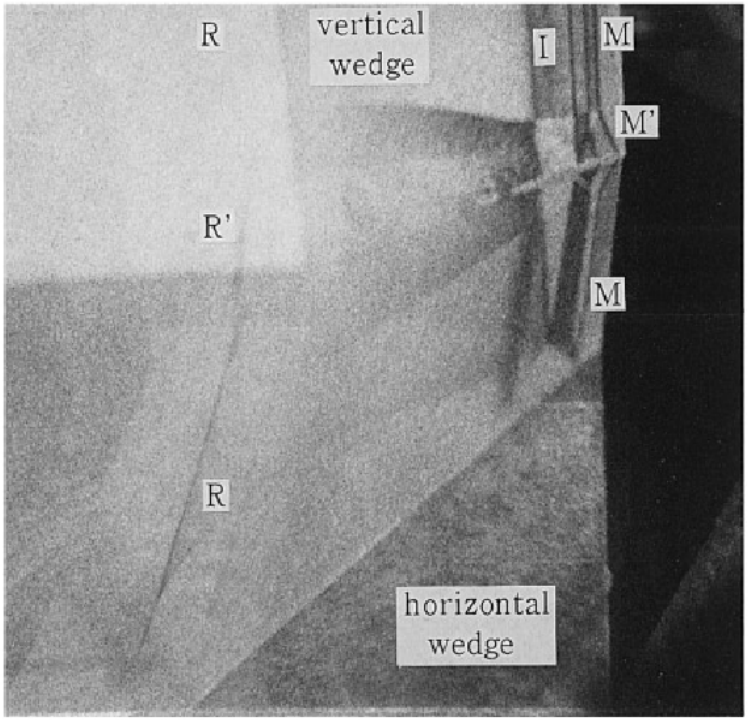
AMR at the shock

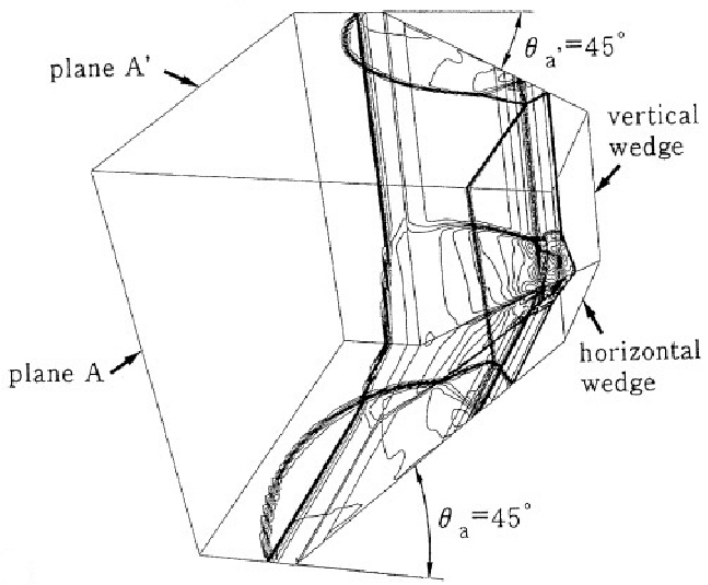


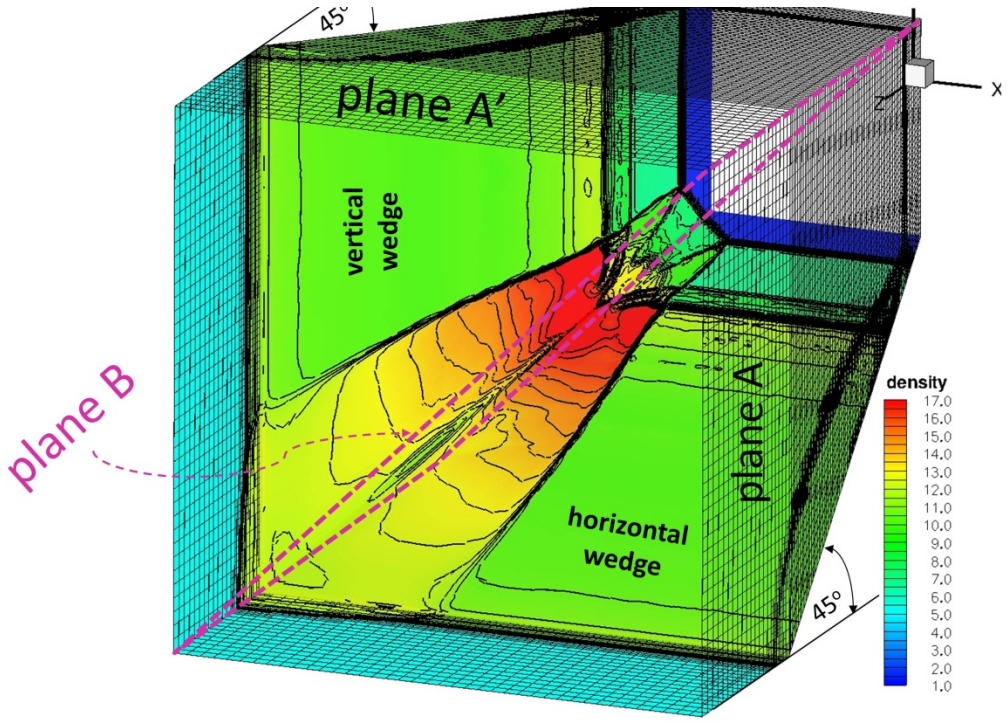
ONERA M6 wing at M = 0.84 and α = 3º



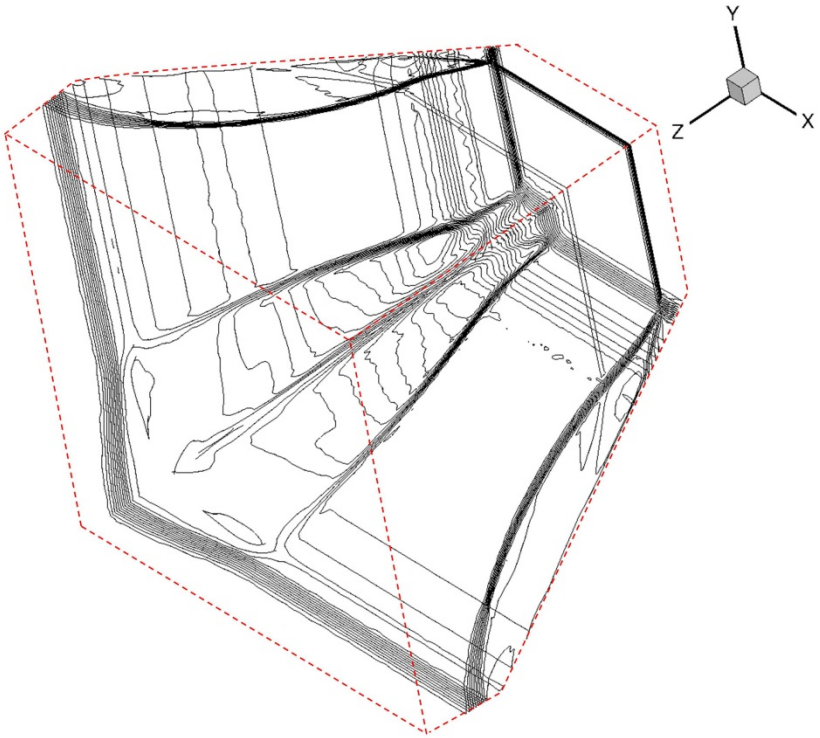
3D double Mach reflection of a moving shock at M = 2.8



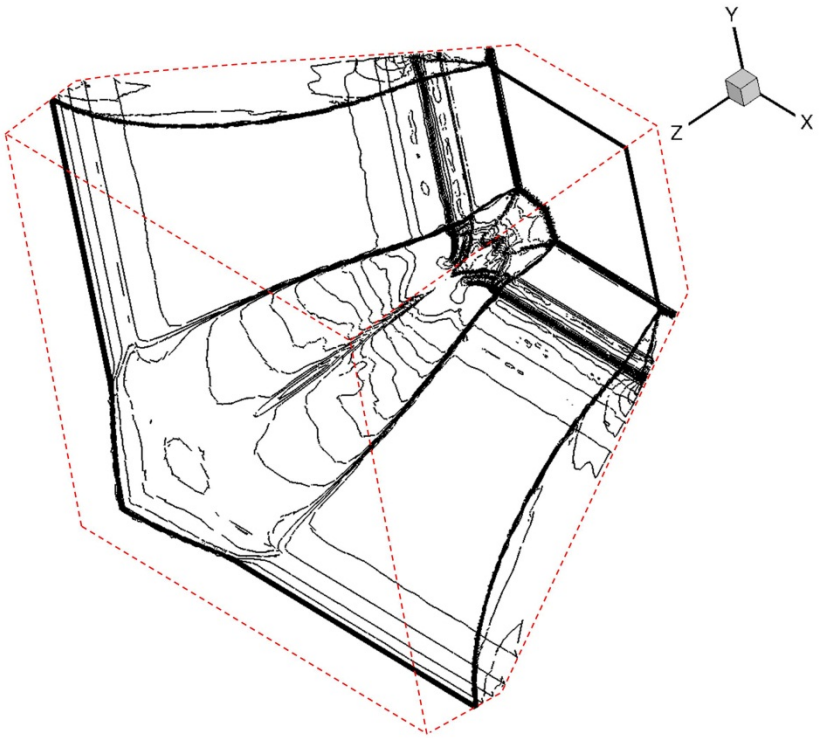




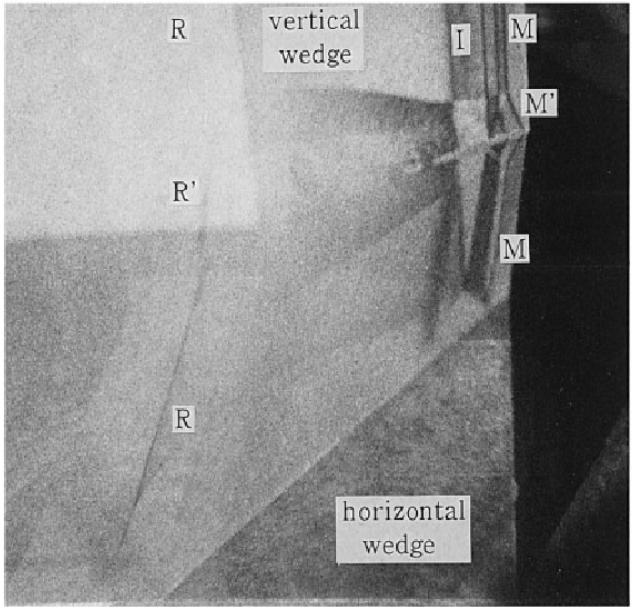
Computed density on a uniform mesh with 8.5×10^5 elements

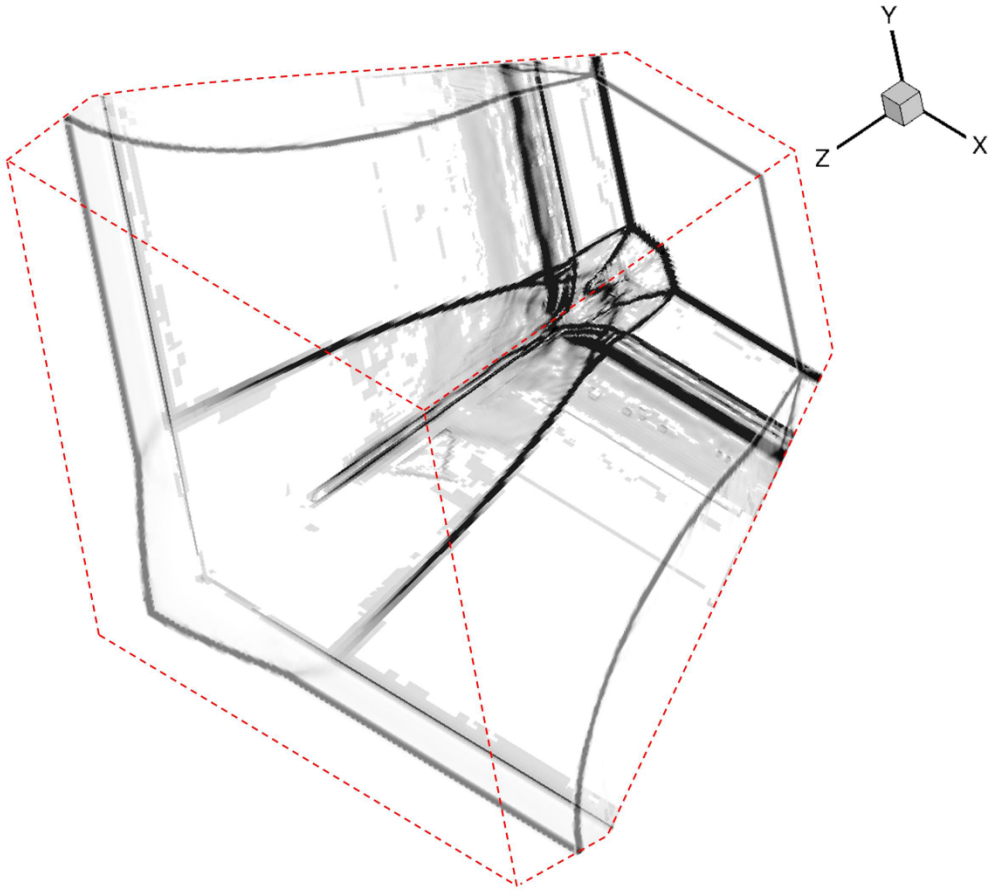


Computed density on a Dynamically adapted mesh with 9×10^5 elements

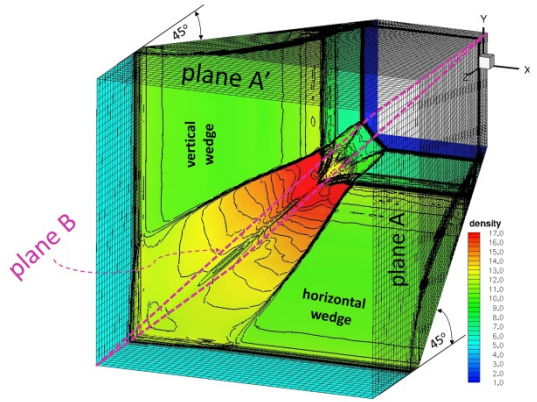


Comparison of numerical Schliren with the experiment

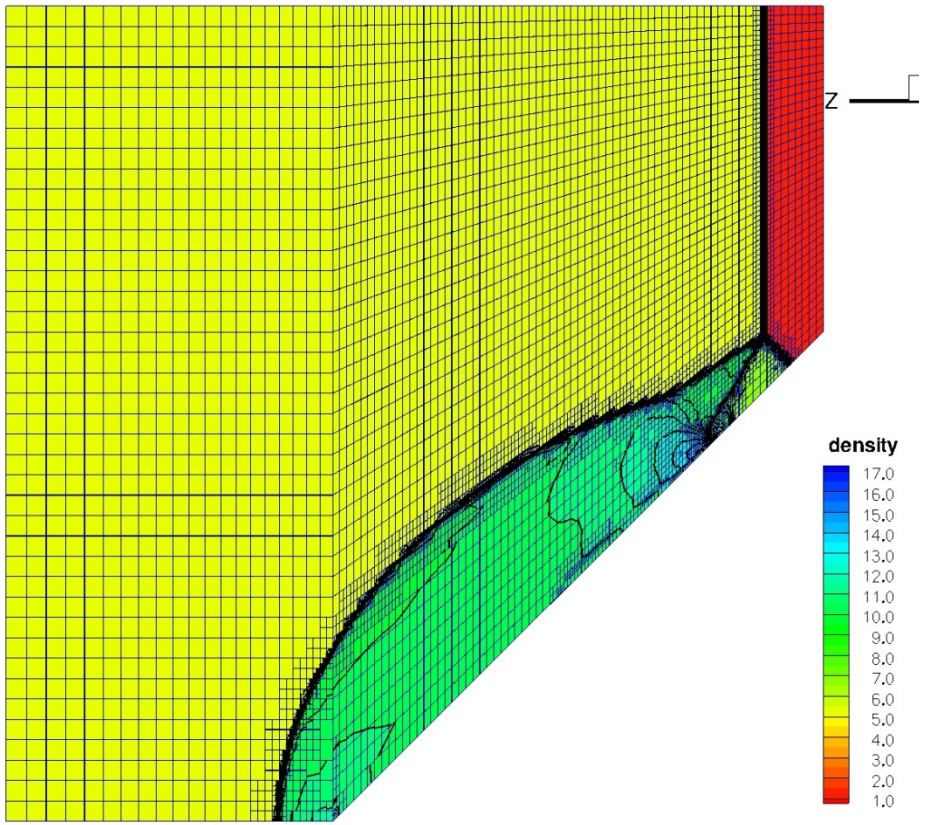




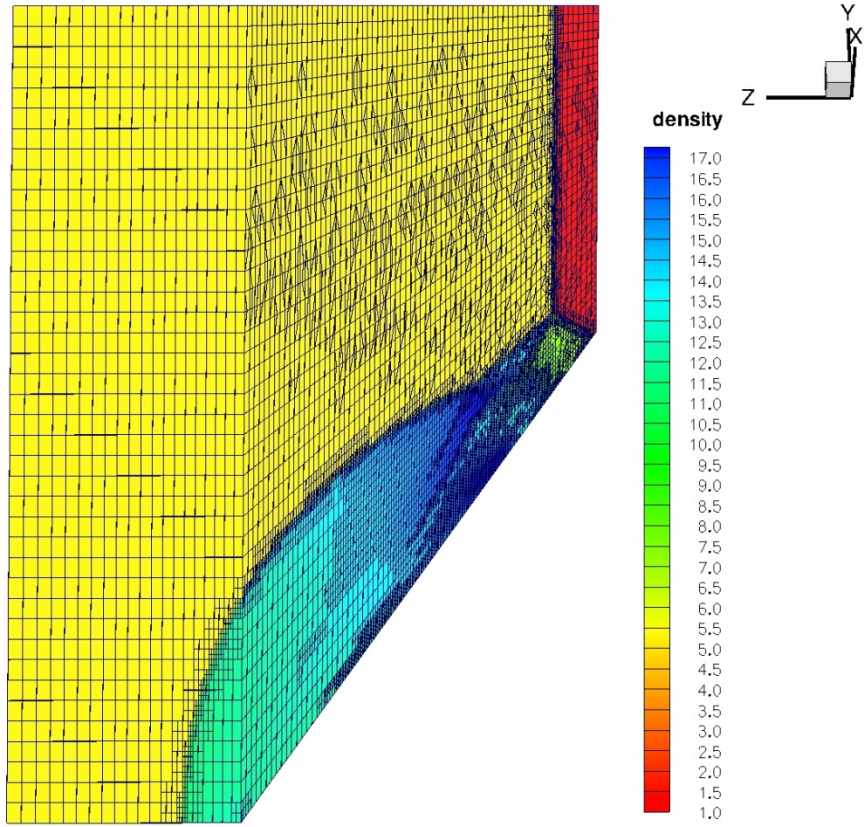
Details of the dynamically adapted mesh



Plane A

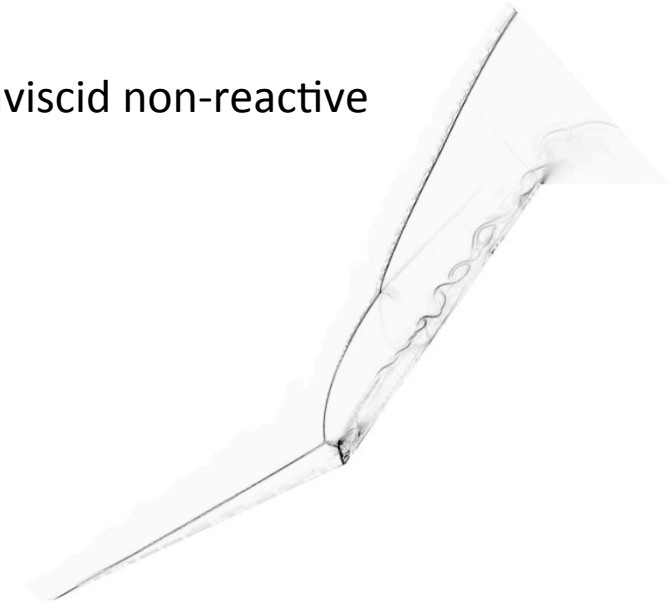


Plane B

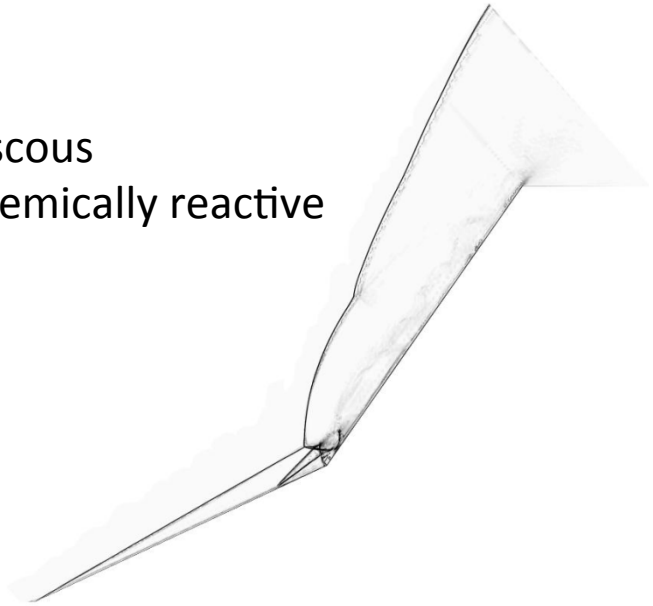


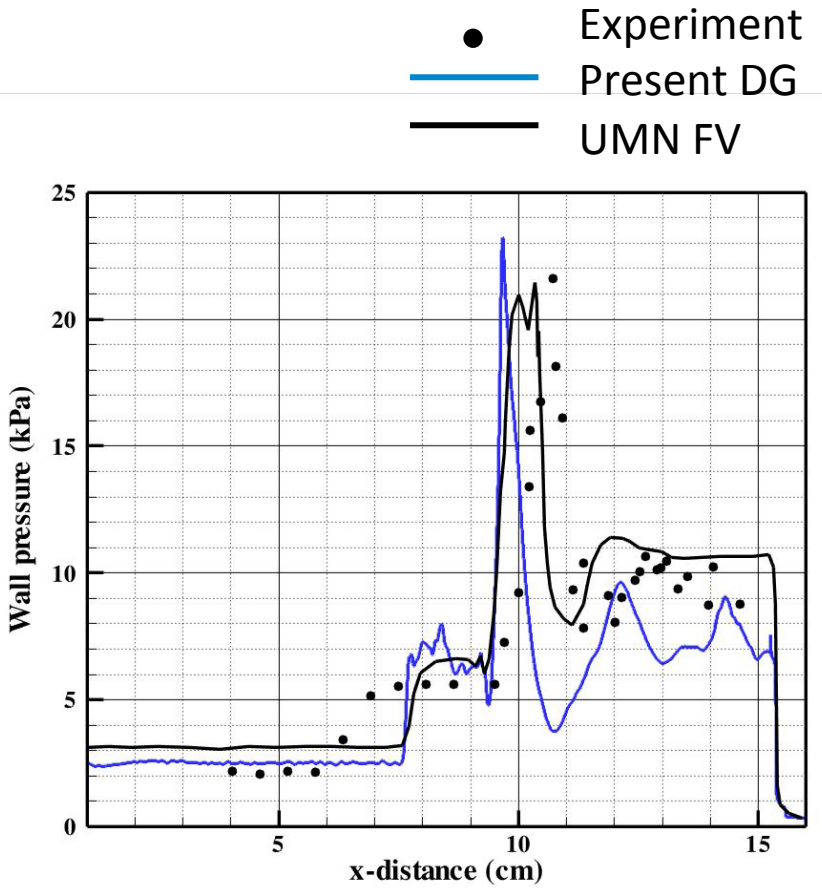
Chemically reactive M = 8 flow over a double cone

Inviscid non-reactive



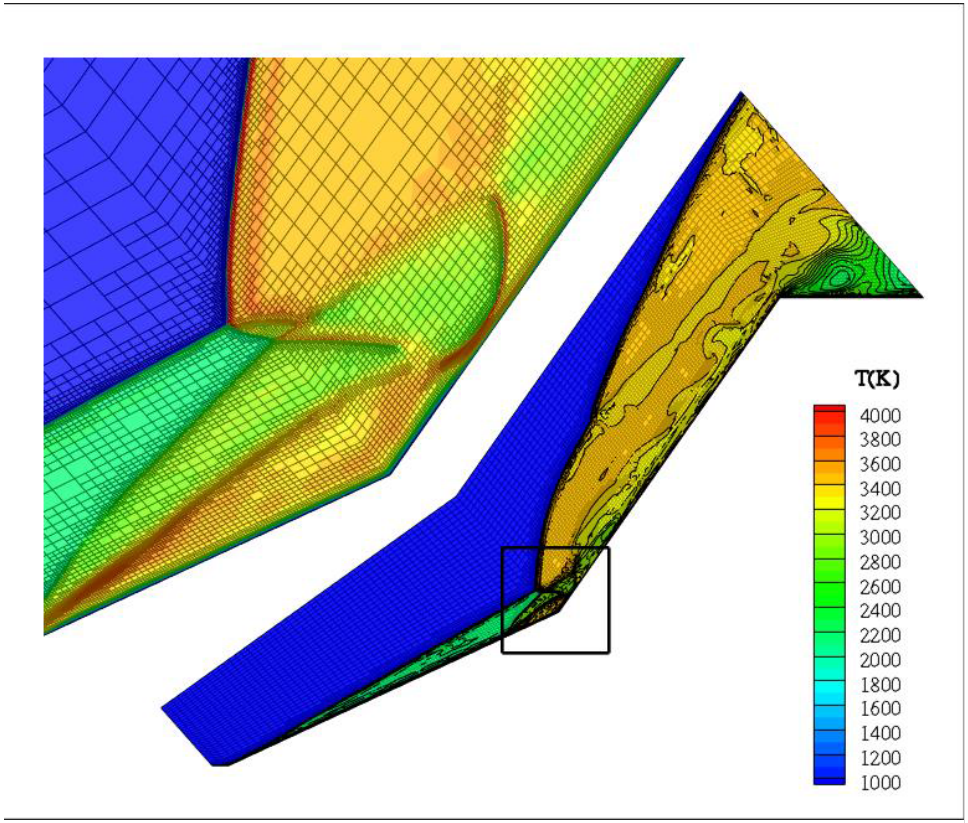
Viscous
Chemically reactive



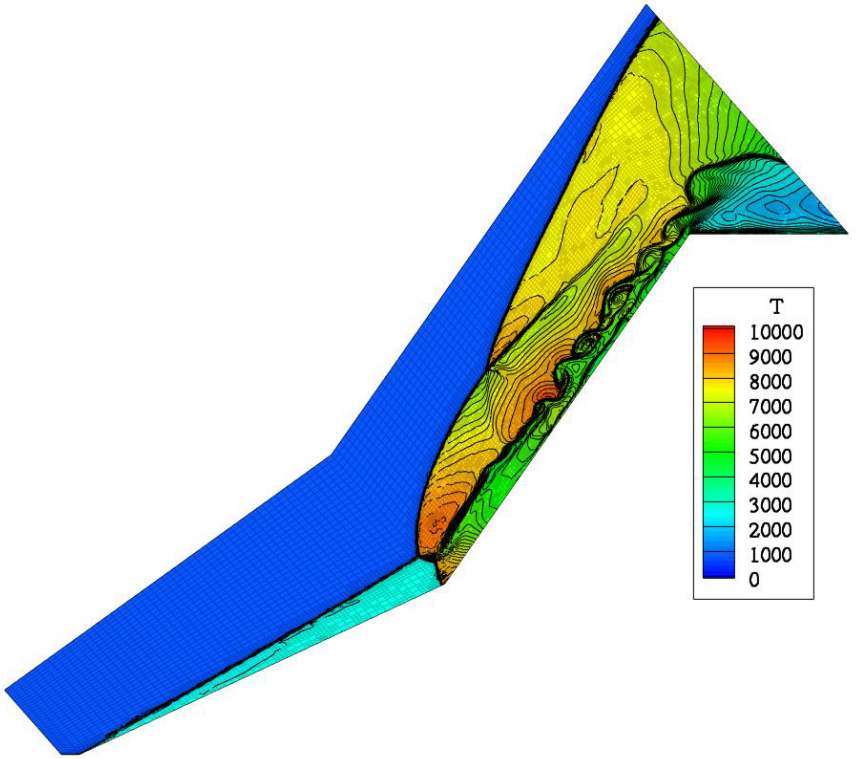


Temperature distributions for reactive and inviscid non-reactive computations

Chemically reactive



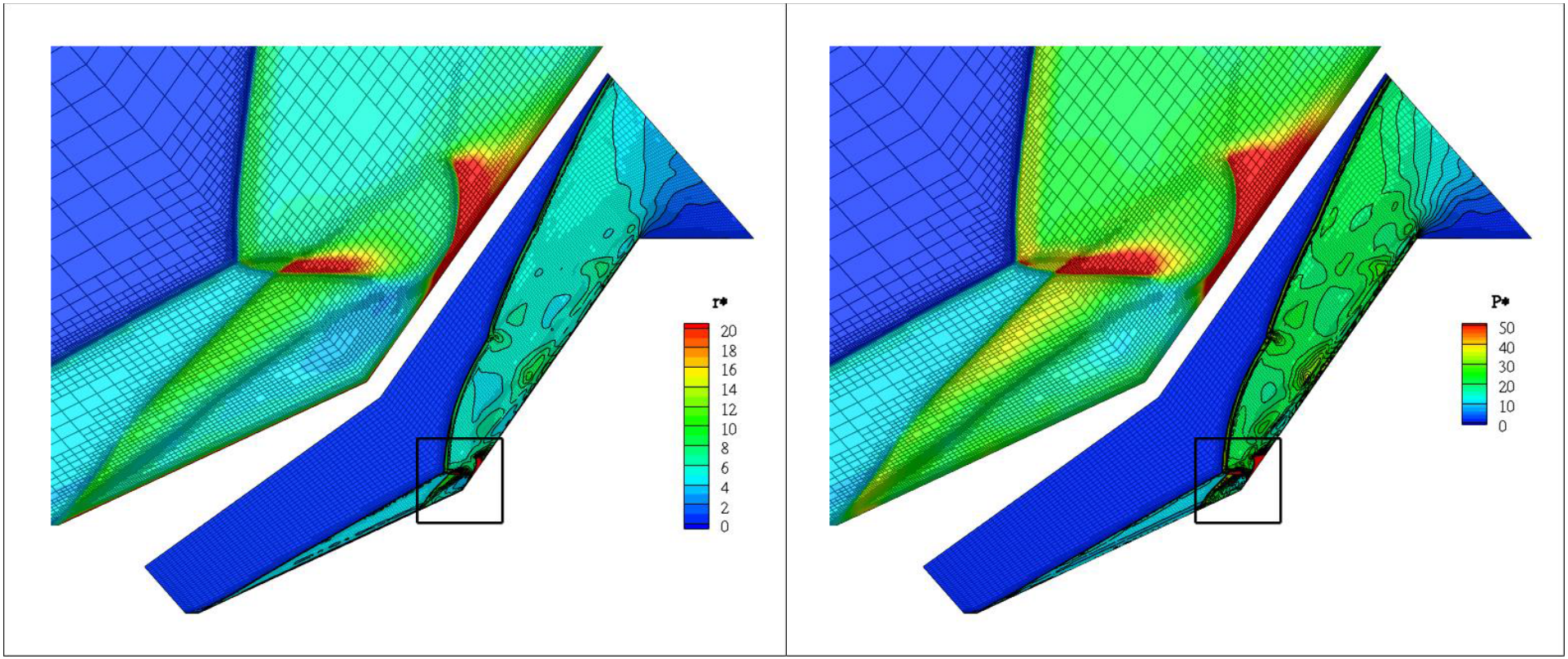
Inviscid non-reactive



Pressure distributions for reactive and non-reactive computations

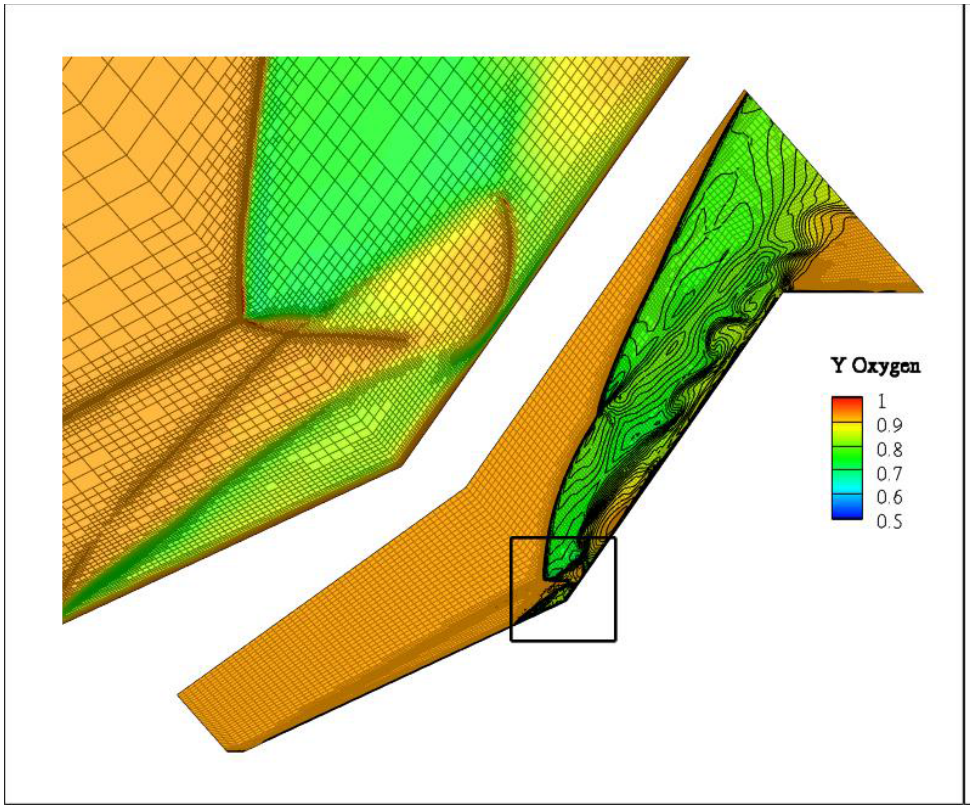
Chemically reactive

Viscous non-reactive

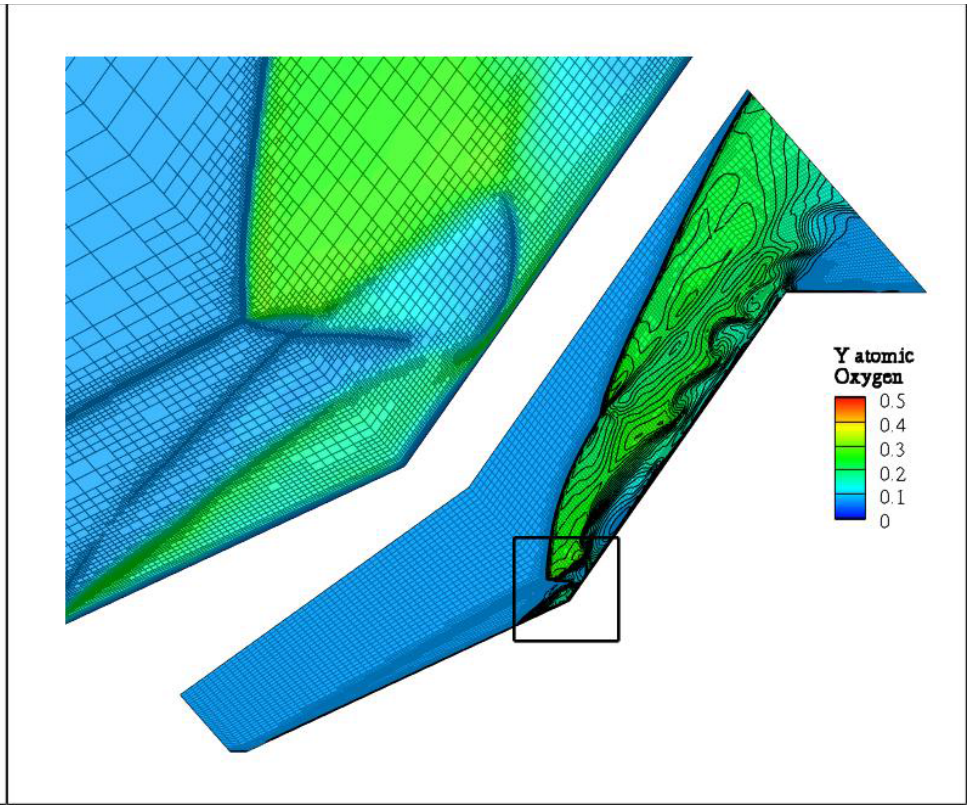


Computed oxygen mass fractions

Distribution of the computed O_2 fraction



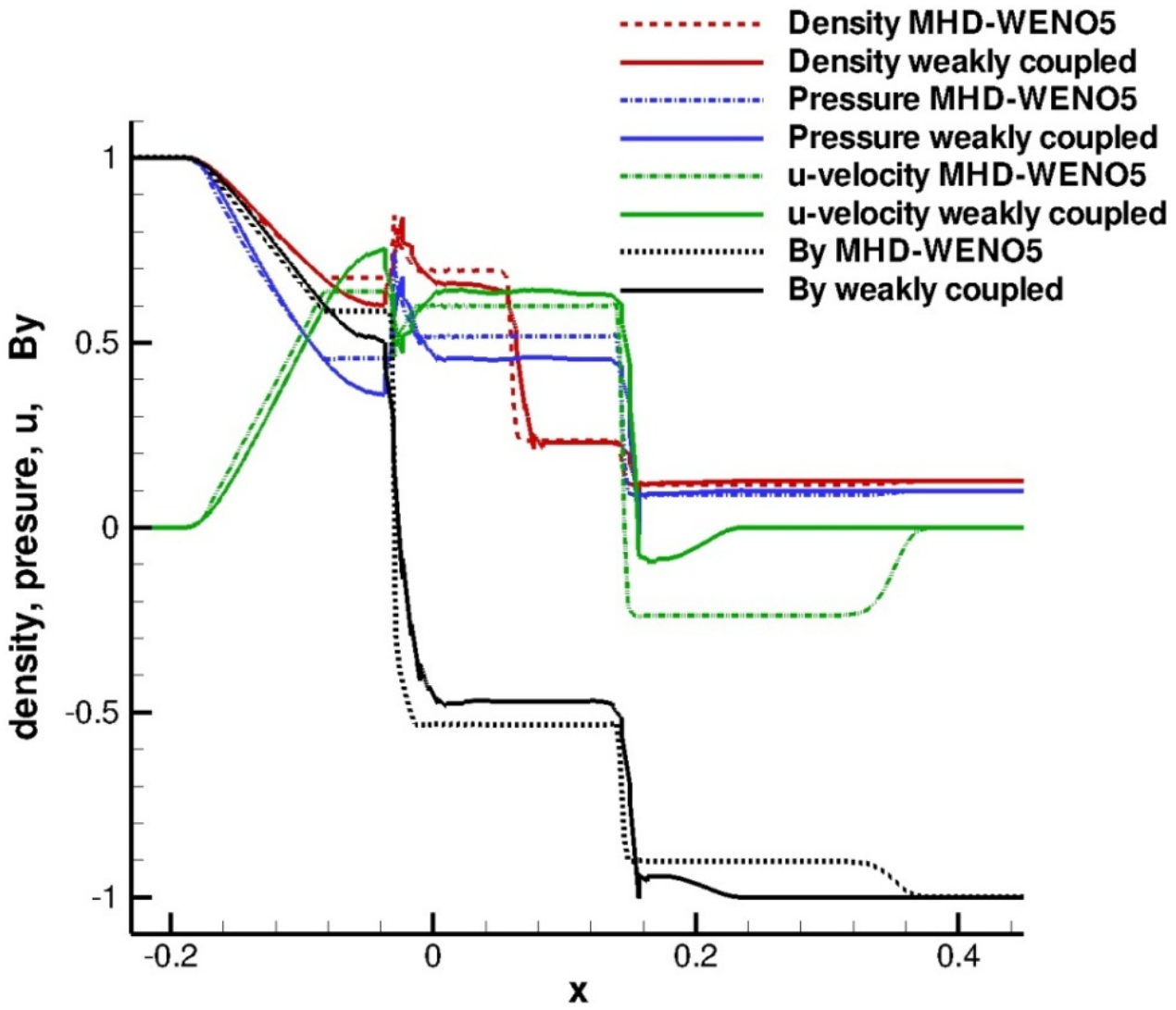
Distribution of the computed O fraction



Effect of segregated time marching

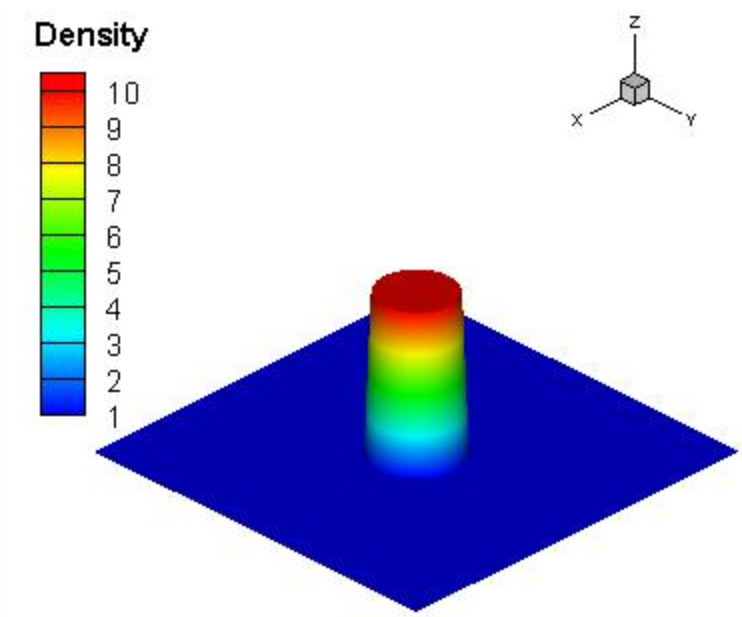
the NS and Maxwell equation systems are marched in time independently and source terms are lagged in time

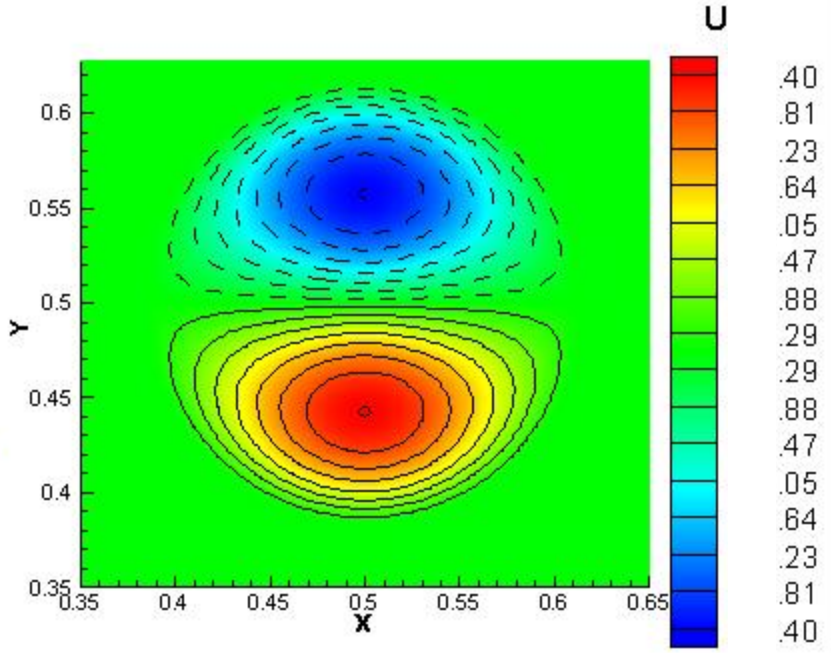
ERAU

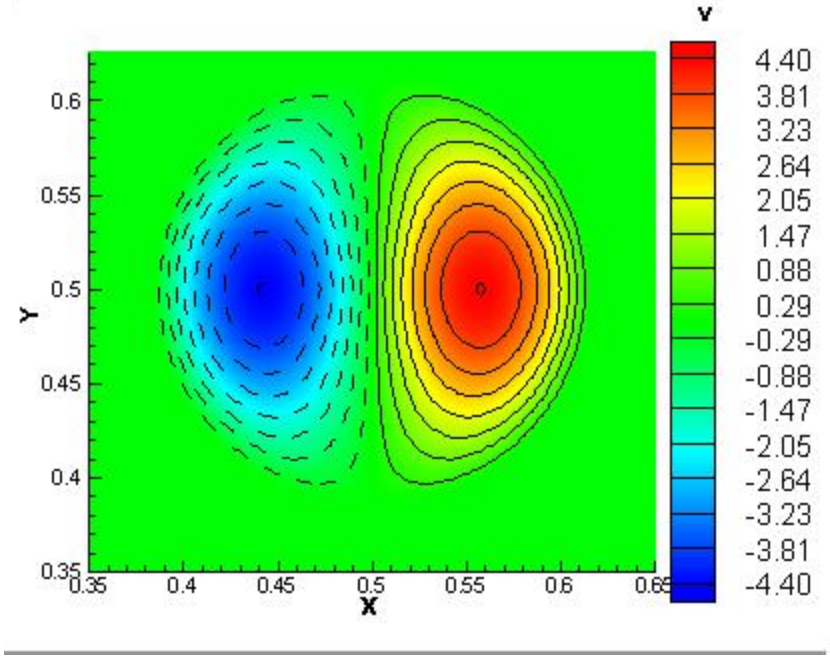


Magnetic Rotor initial conditions

ERAU







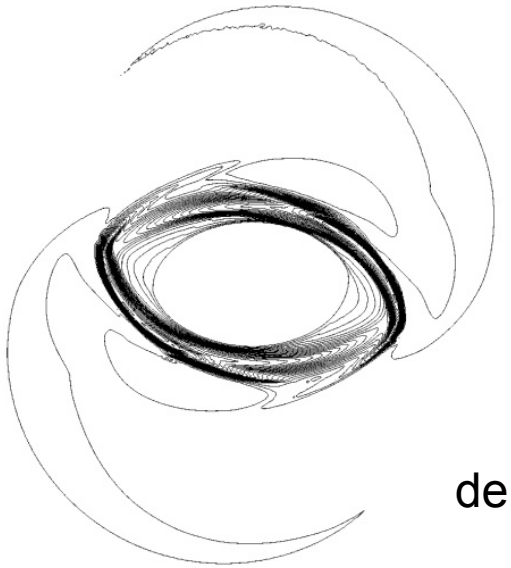
$$p(\mathbf{x}, t=0) = 1.0$$

$$B_x(\mathbf{x}, t=0) = \frac{5}{\sqrt{4\pi}}$$

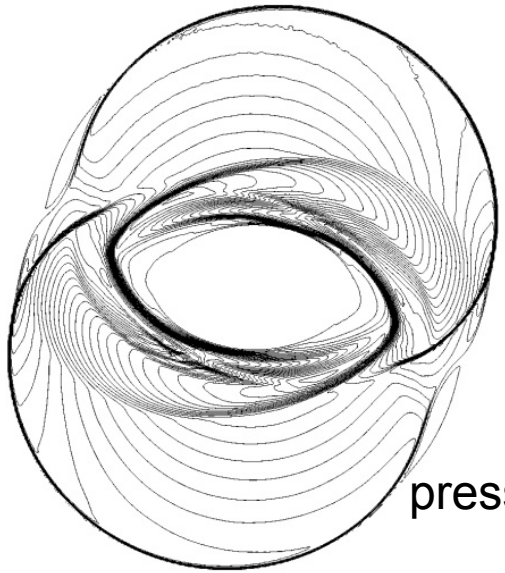
$$B_y(\mathbf{x}, t=0) = 0.0$$

The Rotor Problem

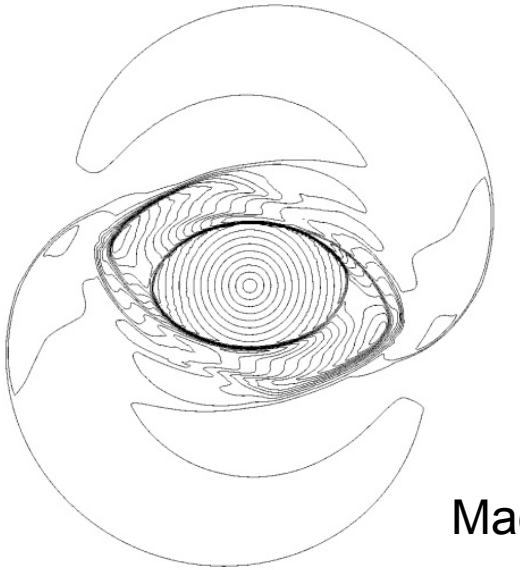
ERAU



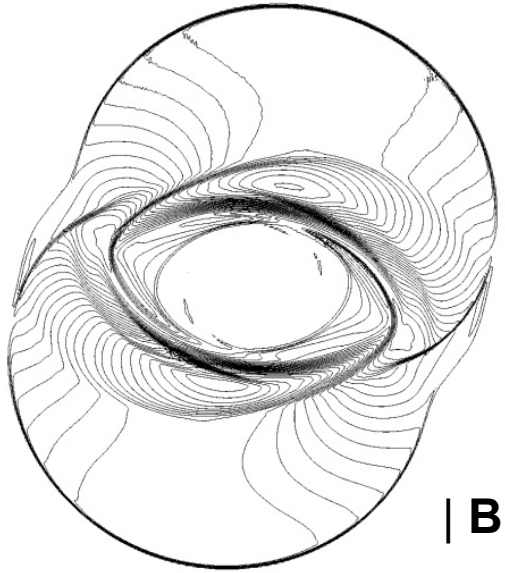
density



pressure



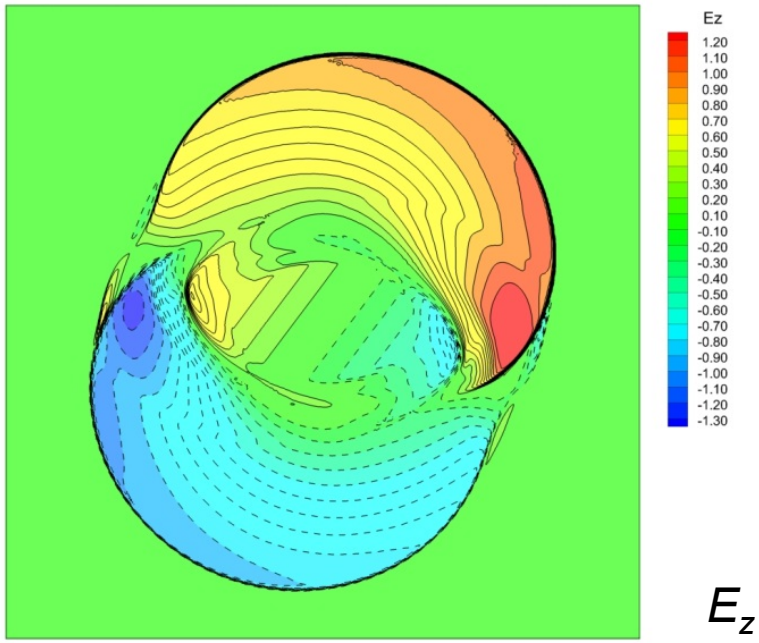
Mach number



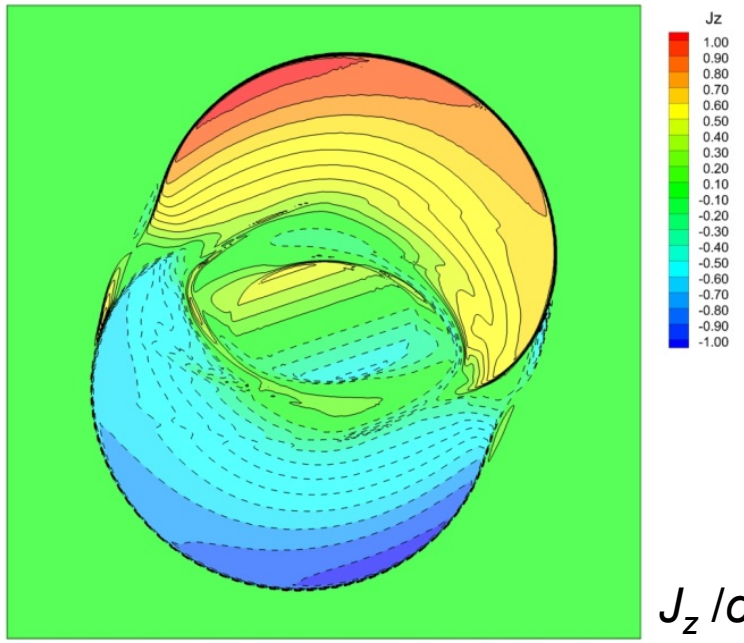
$|\mathbf{B}|^2/2$

The Rotor Problem

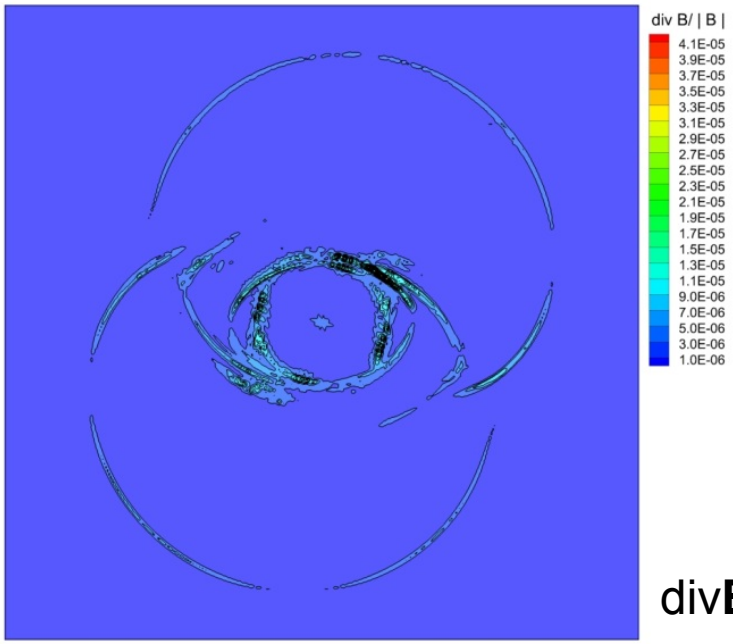
ERAU



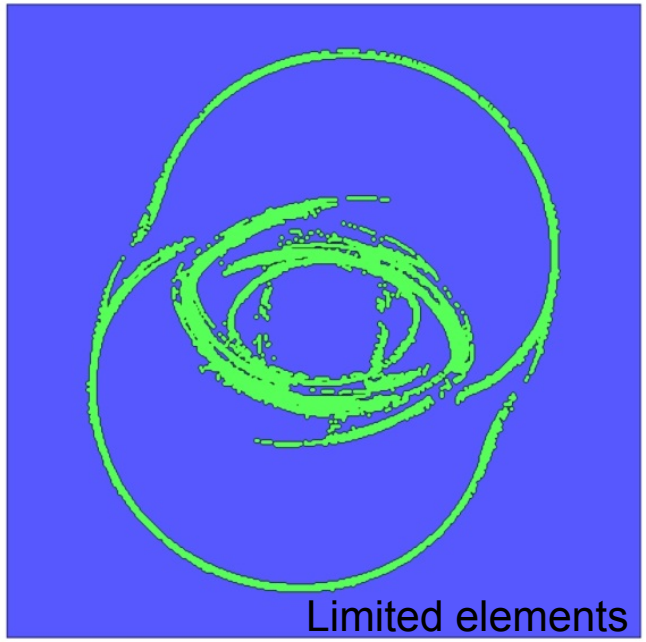
E_z



J_z / σ_e

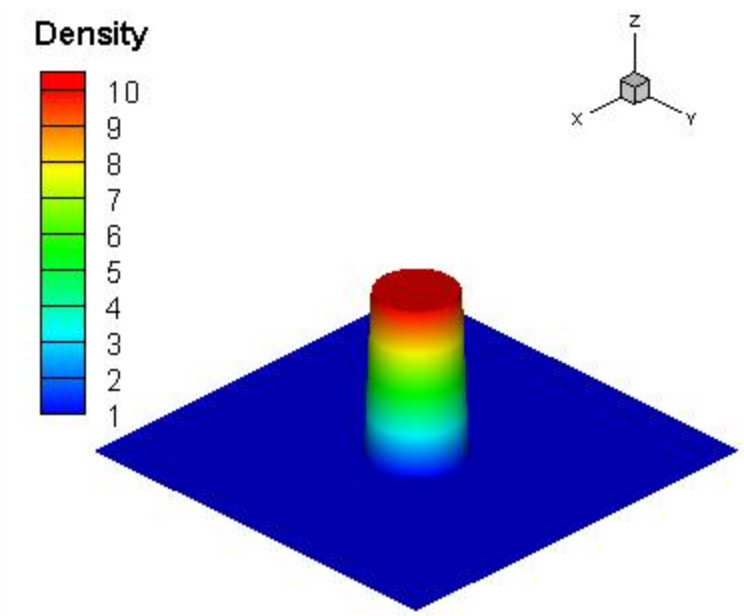


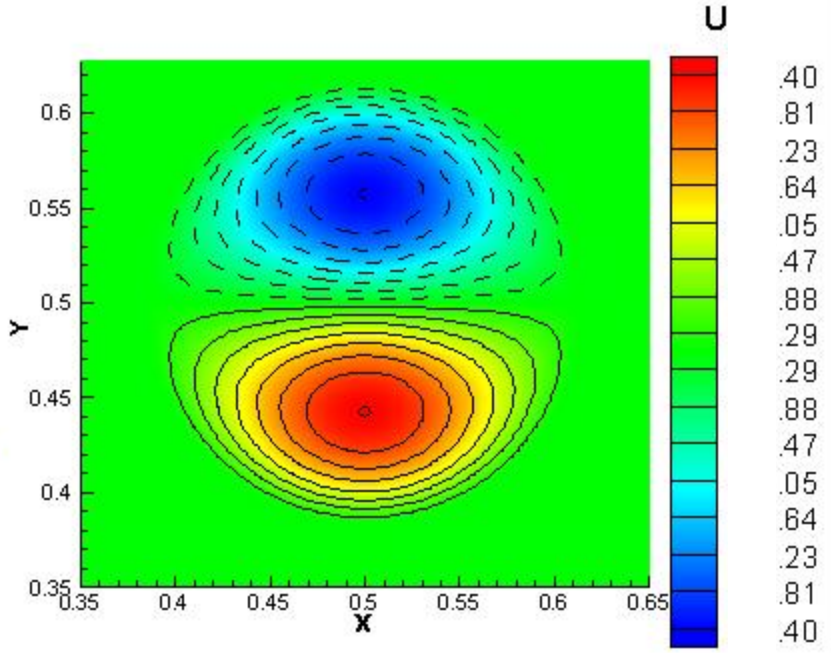
div**B**

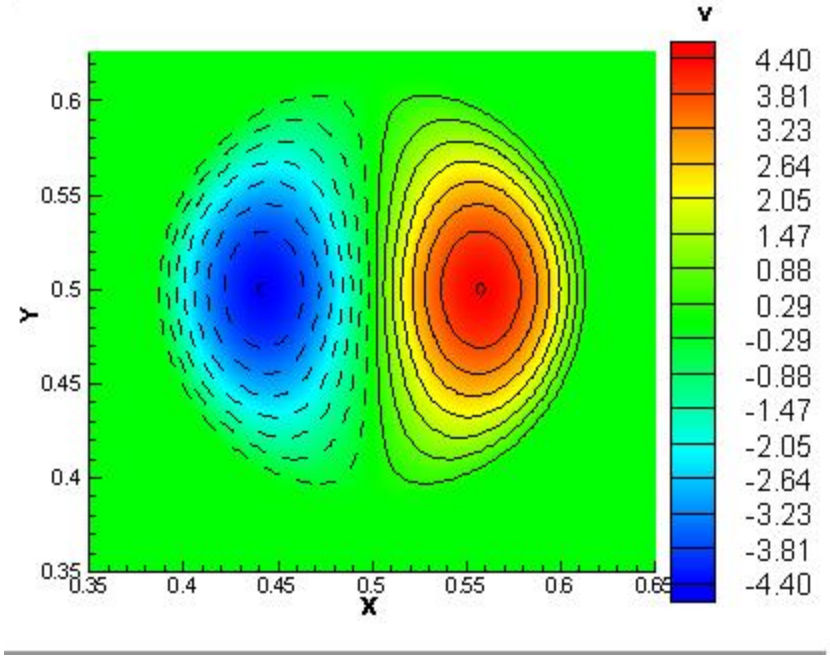


Magnetic Rotor initial conditions

ERAU







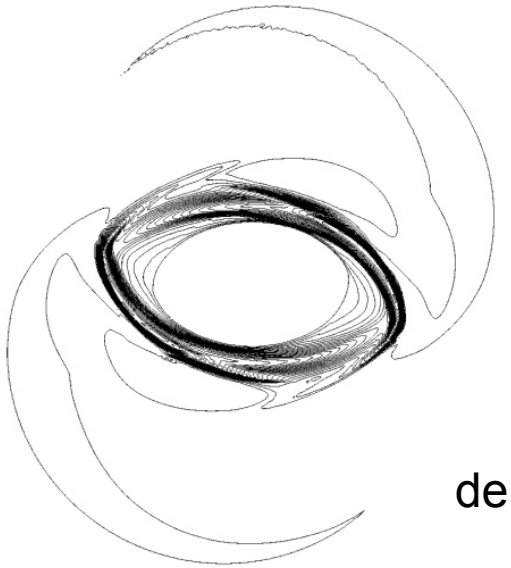
$$p(\mathbf{x}, t=0) = 1.0$$

$$B_x(\mathbf{x}, t=0) = \frac{5}{\sqrt{4\pi}}$$

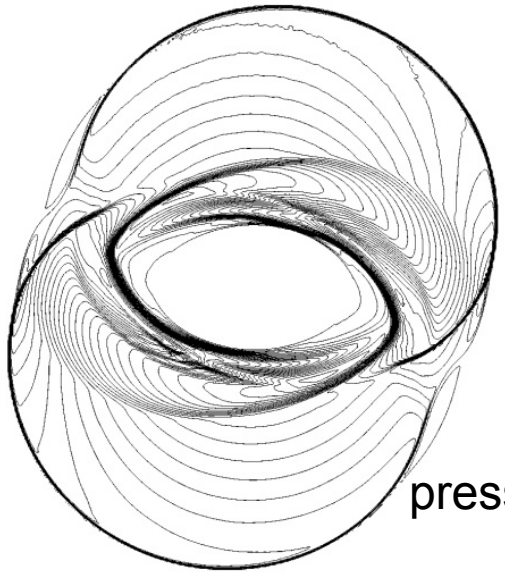
$$B_y(\mathbf{x}, t=0) = 0.0$$

The Rotor Problem

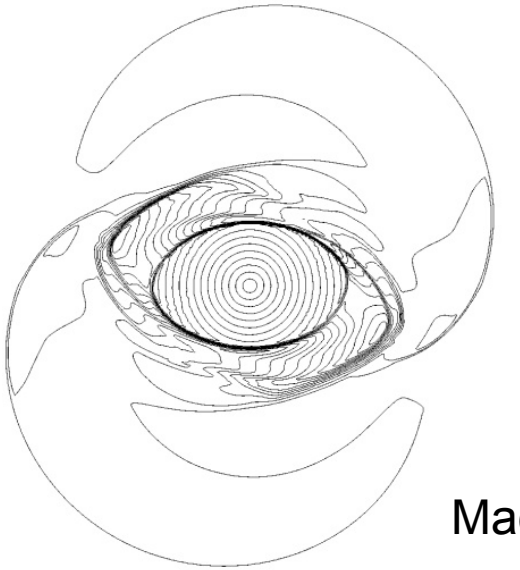
ERAU



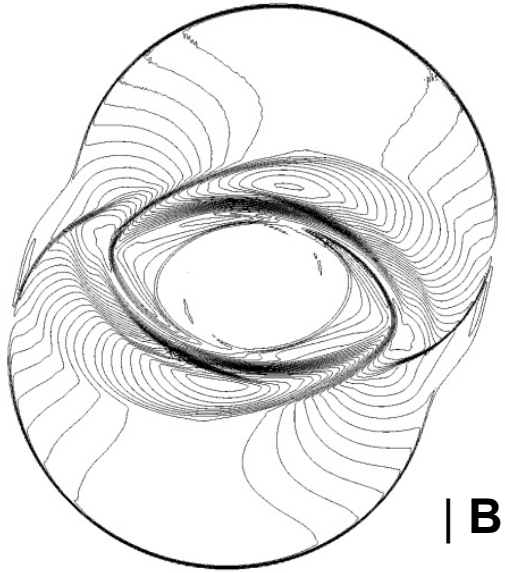
density



pressure



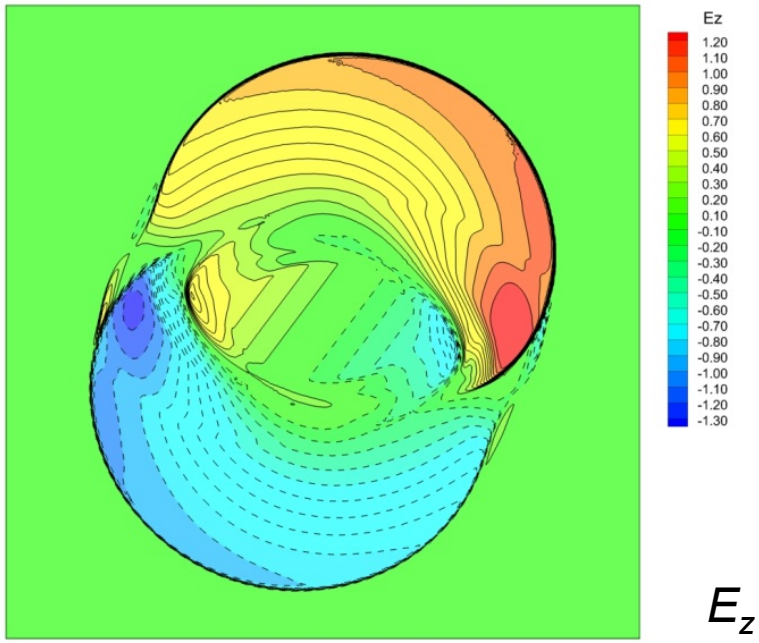
Mach number



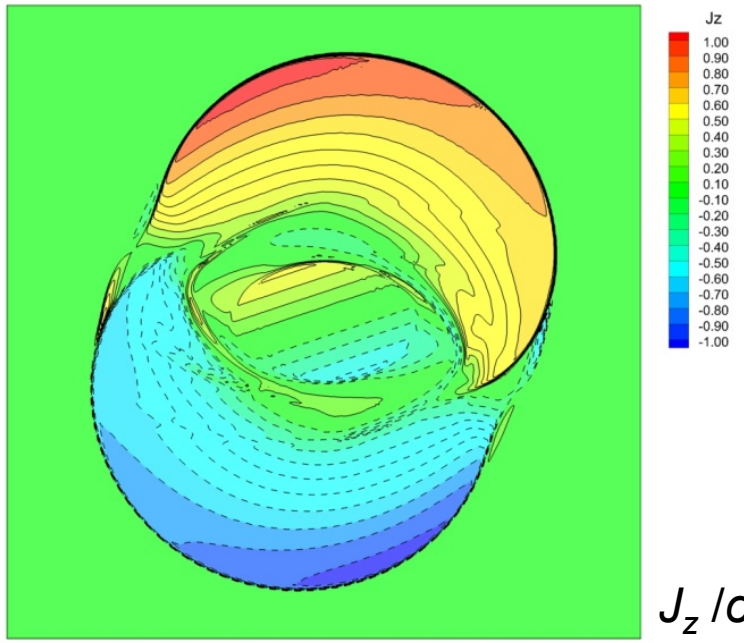
$|\mathbf{B}|^2/2$

The Rotor Problem

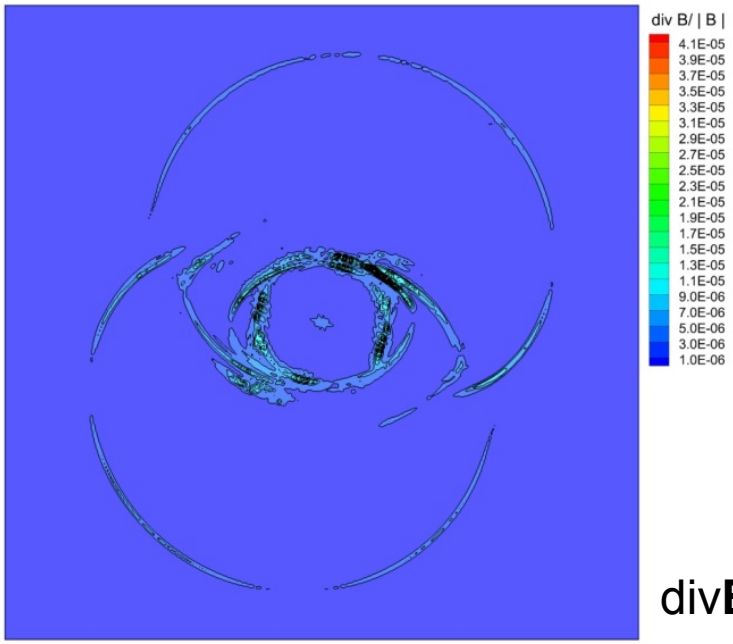
ERAU



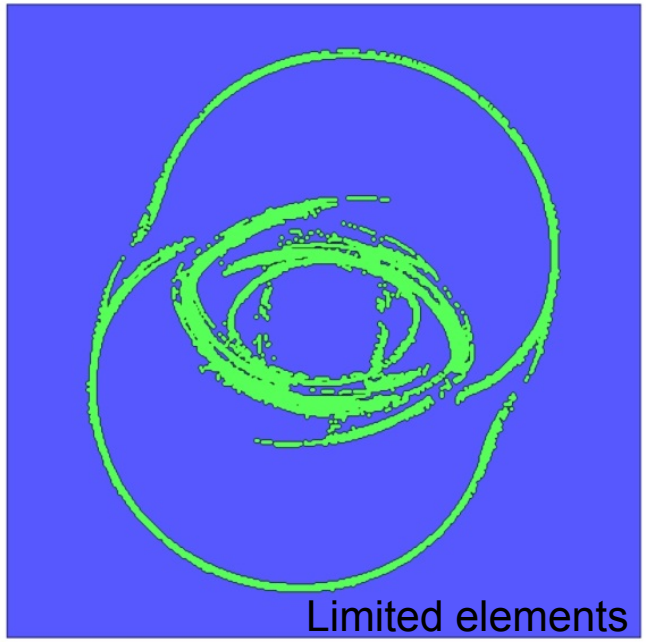
E_z



J_z / σ_e

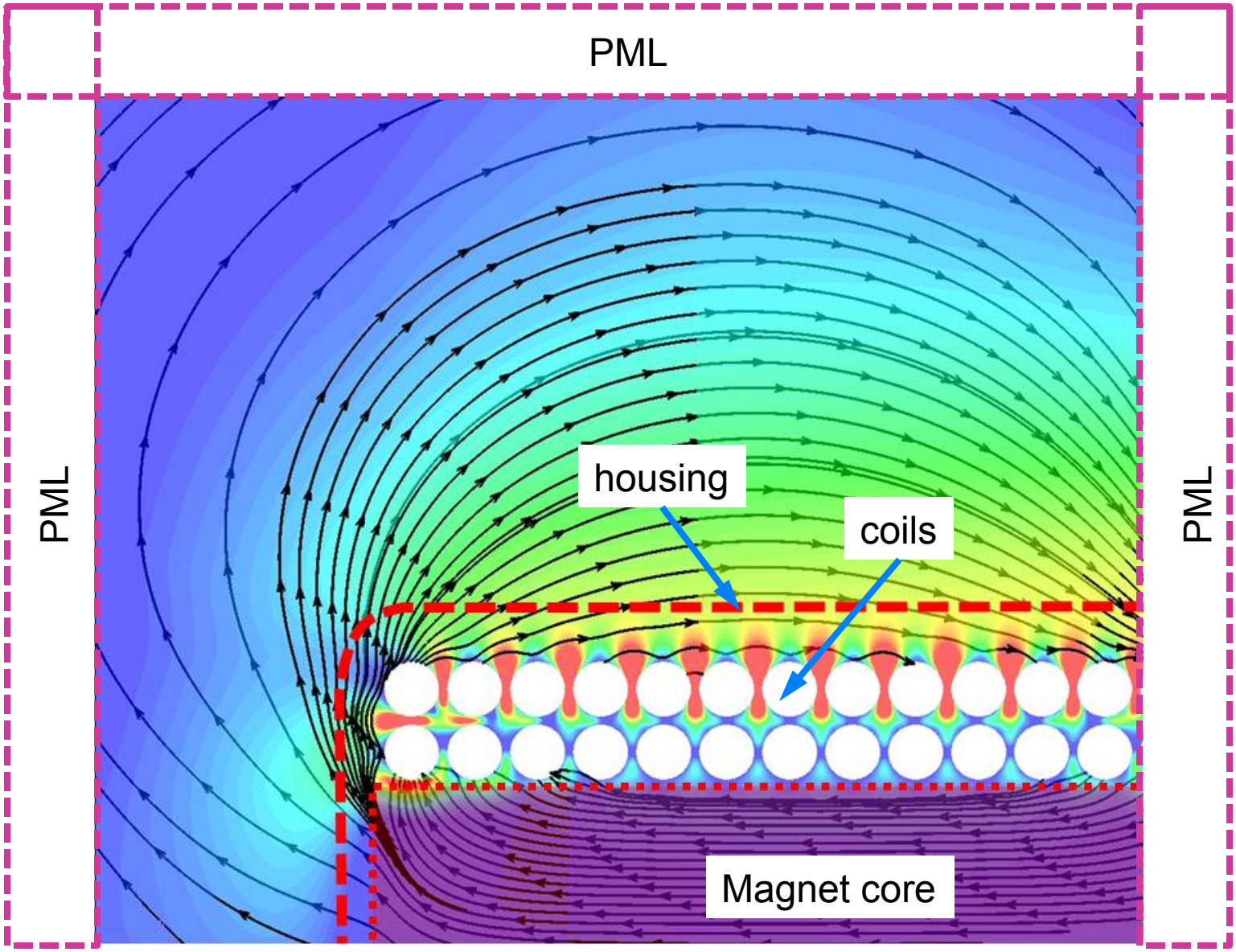


div**B**



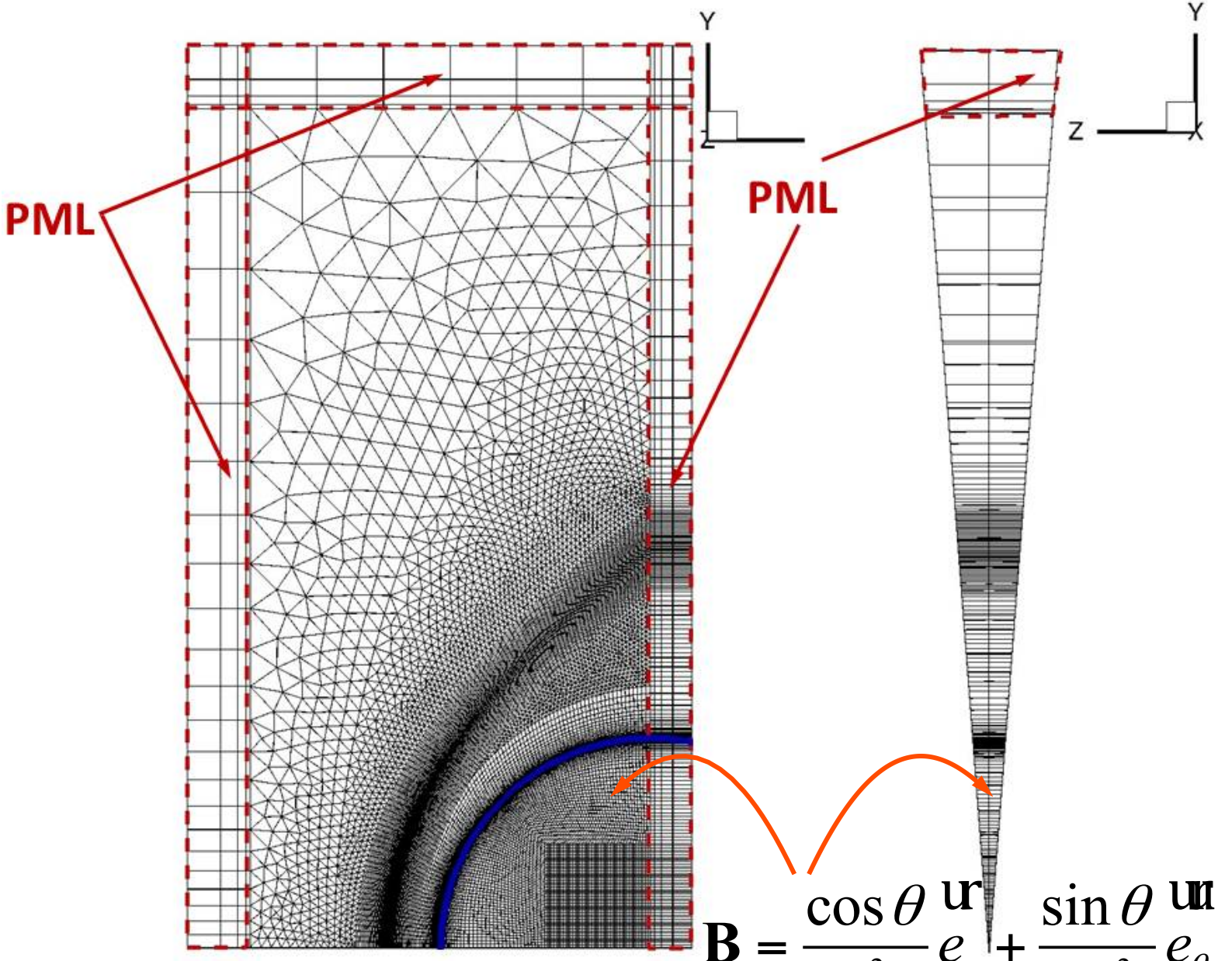
ERAU

Domain with PML regions



ERAU

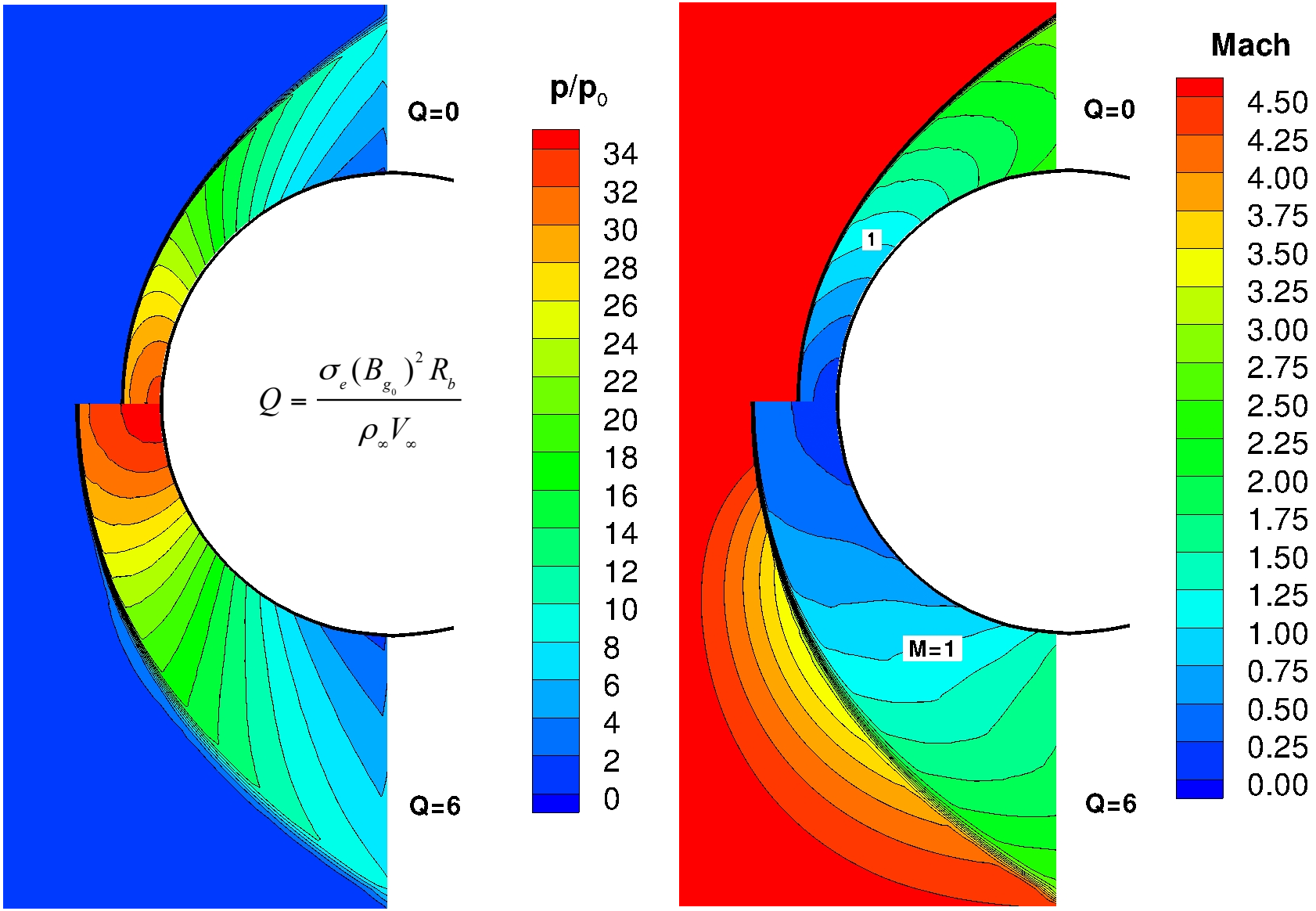
Domain and PML regions for the sphere



$$\mathbf{B} = \frac{\cos\theta}{r^3} e_r + \frac{\sin\theta}{2r^3} e_\theta$$

Increase of shock standoff distance caused by a magnetic dipole at the sphere center

ERAU



Summary

- A unified TVB approach for P1 DG discretizations in unstructured three dimensional meshes (all types of elements) was developed
- Hierarchical TVB limiting for P2 or higher DG discretizations was demonstrated
- Both limiting approaches were applied to unstructured meshes with both implicit and explicit time marching
- The benefits from dynamic adaptive mesh refinement (AMR) for problems with moving shock and unsteady moving flow features was demonstrated.
- Combined dynamic h/p refinement was applied and demonstrated for problems with discontinuities and embedded smooth but complex flow features

